

Robustness Verification of Graph Neural Networks Via Lightweight Satisfiability Testing

Chia-Hsuan Lu¹, Tony Tan², and Michael Benedikt¹

¹ University of Oxford

² University of Liverpool

Abstract. Graph neural networks (GNNs) are the predominant architecture for learning over graphs. As with any machine learning model, an important issue is the detection of adversarial attacks, where an adversary can change the output with a small perturbation of the input. Techniques for solving the *adversarial robustness problem* – determining whether such an attack exists – were originally developed for image classification, but there are variants for many other machine learning architectures. In the case of graph learning, the attack model usually considers changes to the graph structure in addition to or instead of the numerical features of the input, and the state of the art techniques in the area proceed via reduction to constraint solving, working on top of powerful solvers, e.g. for mixed integer programming. We show that it is possible to improve on the state of the art in structural robustness by replacing the use of powerful solvers by calls to efficient *partial solvers*, which run in polynomial time but may be incomplete. We evaluate our tool ROBLIGHT on a diverse set of GNN variants and datasets.

1 Introduction

Graph neural networks (GNNs) have become the dominant model for graph learning, used in many critical applications, such as physical and life sciences [SBV21, DMA⁺15, KMB⁺16].

An important issue in safety of machine learning is *robustness verification*: verifying that small changes to an input do not change the systems' classification. Robustness verification of machine learning systems emerged in image recognition [BK24, LGCR22, LDX⁺24], and has since been explored for a variety of neural architectures. In particular, robustness has been extended to GNNs, where new issues arise as one should consider attacks consisting of small perturbations to the graph structure. Indeed, it has been shown that small structural perturbations can represent effective attacks on common graph learning architectures [FBZA22]. The past literature has considered a variety of models for graph structure perturbation, including the addition and deletion of edges [BG19, ZG20, JSPZ20, LEA25], or even node injection [LZPZ24]. Robustness verification makes sense in the context of every graph learning problem, including node classification and graph classification.

State of the art robustness verification techniques for GNNs are based on two ideas. First one iteratively computes upper and lower bounds to arrive at constraints capturing the existing of a suitable attack. For example the constraint might have variables indexed by edges, representing whether the edge is present or not. Secondly, one solves these constraints, using a general-purpose constraint solver. A canonical example is [HZCM24], which reduces robustness verification to mixed integer linear programming (MIP). The MIP problems are formed by approximating the behaviour of the GNN, and their satisfiability is tested using the MIP solver Gurobi.

The robustness problem is easily seen to be NP-complete, and thus reducing to a generic solver for another NP-hard problem is natural. But it is not clear that these reductions allow the solvers to exploit the structure of the robustness problem. And indeed, despite advances, robustness verification is currently limited to very small GNNs: e.g. 3 layers. Here we take an alternative approach, and make use of *lightweight solvers*. As in prior approaches we iteratively refine approximations to the evaluation of a GNN on a set of graphs obtained from small perturbations, expressing our approximation as a set of constraints. Unlike prior approaches, we test satisfiability of the constraints only approximately, developing our own *partial oracles* that can efficiently determine whether constraints are satisfiable or not, but may return unknown. Although the lightweight solver approach may seem simpler than one based on existing general-purpose solvers, we show that its performance is significantly better than state-of-the-art.

This paper is organised as follows. In Section 2 we introduce the necessary notations and review GNNs and the robustness problem. In Section 3 we present our notion of partial oracles and how

they can be used for robustness analysis. We introduce some optimization strategies in Section 4. We present our experimental results in Section 5. Related work is discussed in Section 6. Finally, we conclude in Section 7. Missing proofs, additional variations of the problems that our tool can handle, and experimental results can be found in the appendix.

2 Preliminaries

Throughout the paper we deal with directed graphs in which each node is associated with a vector of reals.

Definition 1 (Featured graphs). *A featured graph \mathcal{G} , or simply graph for short, is a tuple $\langle V, E, X \rangle$, where V is the set of vertices, $E \subseteq V \times V$ is the set of edges, and $X : V \rightarrow \mathbb{R}^m$ is the input feature mapping.*

For a vertex $v \in V$, we denote the set of incoming neighbors of v , or simply neighbors for short, in a graph \mathcal{G} by $\mathcal{N}_{\mathcal{G}}(v)$, that is

$$\mathcal{N}_{\mathcal{G}}(v) := \{u \in V \mid (u, v) \in E\}.$$

We need to analyze the behavior of a network on a collection of graphs obtained through edge insertions and deletions. We will abstract the inputs using the following notion of incomplete graphs, a variant of the general notion of incomplete dataset in database theory [AHV95]:

Definition 2 (Incomplete graphs). *An incomplete graph \mathcal{H} is a tuple $\langle V, E, E^{\text{Unk}}, E^{\text{Non}}, X \rangle$, where V is the set of vertices, E is the set of normal edges, E^{Unk} is the set of unknown edges, E^{Non} is the set of non-edges, and $X : V \rightarrow \mathbb{R}^m$ is the input feature mapping, satisfying that E , E^{Unk} , and E^{Non} form a partition of $V \times V$.*

For a vertex $v \in V$, we denote the set of incoming normal and incoming unknown neighbors of v in \mathcal{G} by $\mathcal{N}_{\mathcal{G}}^{\text{Norm}}(v)$ and $\mathcal{N}_{\mathcal{G}}^{\text{Unk}}(v)$.

We will sometimes abuse notation by treating a graph as a special kind of incomplete graph where $E^{\text{Unk}} = \emptyset$.

We denote the set of all incomplete graphs with vertex set V and input feature mapping X by $\mathfrak{H}_{V,X}$. We denote by $\mathfrak{G}_{V,X}$ the subset of “normal graphs” – those with no unknown edges. We will use \mathcal{H} to denote an incomplete graph, and often assume a vertex set V and feature map X .

Incomplete graphs on the same vertex set have a natural “information order”, a partial order relation on the set $\mathfrak{H}_{V,X}$.

Definition 3 (Refinement). *For incomplete graphs $\mathcal{H}_1, \mathcal{H}_2 \in \mathfrak{H}_{V,X}$, we say that \mathcal{H}_2 refines \mathcal{H}_1 , denoted by $\mathcal{H}_2 \subseteq \mathcal{H}_1$, if:*

$$E_2 \subseteq E_1 \cup E_1^{\text{Unk}}, \quad E_2^{\text{Unk}} \subseteq E_1^{\text{Unk}}, \quad \text{and} \quad E_2^{\text{Non}} \subseteq E_1^{\text{Non}} \cup E_1^{\text{Unk}}.$$

Intuitively, $\mathcal{H}_2 \subseteq \mathcal{H}_1$ if and only if \mathcal{H}_2 can be obtained from \mathcal{H}_1 through a sequence of converting an unknown edge into a normal edge and converting an unknown edge into a non-edge. Featured graphs are the minimal elements of this order:

Definition 4 (Completion). *For an incomplete graph $\mathcal{H} \in \mathfrak{H}_{V,X}$, the completions of \mathcal{H} , denoted by $\text{COMP}(\mathcal{H})$, is the set of graphs that refine \mathcal{H} .*

It is easy to see that $\mathcal{H}_2 \subseteq \mathcal{H}_1$ if and only if $\text{COMP}(\mathcal{H}_2) \subseteq \text{COMP}(\mathcal{H}_1)$.

Definition 5 (Grounding). *For an incomplete graph $\mathcal{H} \in \mathfrak{H}_{V,X}$, and a graph $\mathcal{G} \in \mathfrak{G}_{V,X}$, the grounding \mathcal{G}' of \mathcal{H} to \mathcal{G} is the completion of \mathcal{H} obtained by the procedure: for every edge $e \in E^{\text{Unk}}$, if e is an edge in \mathcal{G} , then e is converted to a normal edge in \mathcal{G}' ; otherwise, if e is not an edge in \mathcal{G} , then e is converted to a non-edge in \mathcal{G}' .*

Intuitively, grounding of \mathcal{H} to \mathcal{G} is the completion of \mathcal{H} that is closest to \mathcal{G} . We will formalize this once we define a notion of distance.

We will also need a way of introducing incompleteness:

Definition 6 (Relaxation). For a graph $\mathcal{G} \in \mathfrak{H}_{V,X}$ and a set $E_p \subseteq V \times V$ the relaxation of \mathcal{G} by E_p , denoted by $\mathcal{H}_{\mathcal{G}, E_p}$, is the incomplete graph obtained from \mathcal{G} by making all the edges in E_p unknown, and subtracting off any edges in E_p from both the edge set E and the set of non-edges.

Next, we define the notion of distance on the set of incomplete graphs.

Definition 7 (Distance). For incomplete graphs $\mathcal{H}_1, \mathcal{H}_2 \in \mathfrak{H}_{V,X}$, for vertices $v, u \in V$, we say that (v, u) is inconsistent between \mathcal{H}_1 and \mathcal{H}_2 if either:

- $(v, u) \in E_1$ and $(v, u) \in E_2^{\text{Non}}$; or
- $(v, u) \in E_1^{\text{Non}}$ and $(v, u) \in E_2$.

The distance between \mathcal{H}_1 and \mathcal{H}_2 , denoted by $\text{dist}(\mathcal{H}_1, \mathcal{H}_2)$ is defined as

$$\text{dist}(\mathcal{H}_1, \mathcal{H}_2) := |\{(v, u) \in V \times V \mid (v, u) \text{ is inconsistent between } \mathcal{H}_1 \text{ and } \mathcal{H}_2\}|.$$

Note that the distance between \mathcal{H}_1 and \mathcal{H}_2 can equivalently be defined to be the minimum of the distances between a completion of \mathcal{H}_1 and a completion of \mathcal{H}_2 .

One can check that, for all incomplete graphs $\mathcal{H}, \mathcal{H}_1, \mathcal{H}_2 \in \mathfrak{H}_{n,X}$ 1. $\text{dist}(\mathcal{H}, \mathcal{H}) = 0$. 2. $\text{dist}(\mathcal{H}_1, \mathcal{H}_2) = \text{dist}(\mathcal{H}_2, \mathcal{H}_1)$. 3. $\mathcal{H}_2 \subseteq \mathcal{H}_1$ implies $\text{dist}(\mathcal{H}_2, \mathcal{H}) \geq \text{dist}(\mathcal{H}_1, \mathcal{H})$.

A way to achieve the minimal distance from a graph to an incomplete graph is to use the grounding:

Lemma 1. For every incomplete graph $\mathcal{H} \in \mathfrak{H}_{V,X}$ and graph $\mathcal{G} \in \mathfrak{H}_{V,X}$, letting \mathcal{G}' be the grounding of \mathcal{H} to \mathcal{G} , it holds that $\text{dist}(\mathcal{G}', \mathcal{G}) = \text{dist}(\mathcal{H}, \mathcal{G})$.

The incomplete graph generated by relaxing a graph \mathcal{G} has distance zero to the graph, since \mathcal{G} is one of its completions:

Lemma 2. For every graph $\mathcal{G} \in \mathfrak{H}_{V,X}$ and every set E_p of pairs of nodes, \mathcal{G} is a completion of its relaxation with respect to E_p , and hence $\text{dist}(\mathcal{H}_{\mathcal{G}, E_p}, \mathcal{G}) = 0$.

2.1 Graph Neural Networks

Graph neural networks are neural network architectures that can be used for a variety of machine learning tasks, including node-level classification: in this context, they take a featured graph as input and output predictions for each node. We focus on *message-passing neural networks* [GSR⁺17, HYL17], which are architectures with a fixed number of layers. Following the literature on robustness of GNNs [HZCM24], we use a variation that involves directed graphs, with aggregation over incoming nodes. We discuss modifications for undirected graphs and for graph-level classification in the appendix.

At each layer, the network produces a new feature vector for each node, aggregating the previous-layer features from its incoming neighbors and applying a feedforward neural networks to the node's own previous-layer features.

Definition 8 (Graph neural network). An L -layer graph neural network \mathcal{A} consists of a sequence of dimensions $d^{(0)}, d^{(1)}, \dots, d^{(L)} \in \mathbb{N}^+$, an aggregation function $\text{aggr} \in \{\text{sum}, \text{max}, \text{mean}\}$, and, for each $1 \leq \ell \leq L$, learnable coefficient matrices $\mathbf{C}^{(\ell)}, \mathbf{A}^{(\ell)} \in \mathbb{R}^{d^{(\ell)} \times d^{(\ell-1)}}$ together with bias vectors $\mathbf{b}^{(\ell)} \in \mathbb{R}^{d^{(\ell)}}$.

Definition 9 (Computation of a GNN). For an L -layer GNN \mathcal{A} and a featured graph $\mathcal{G} \in \mathfrak{G}_{V,X}$, the computation of \mathcal{A} on \mathcal{G} is a sequence of features $\xi_{\mathcal{G}}^{(\ell)}(v)$ for $0 \leq \ell \leq L$ and $v \in V$. For $\ell = 0$, we set $\xi_{\mathcal{G}}^{(0)}(v) := X(v)$. For $1 \leq \ell \leq L$,

$$\xi_{\mathcal{G}}^{(\ell)}(v) := \text{ReLU} \left(\mathbf{C}^{(\ell)} \cdot \xi_{\mathcal{G}}^{(\ell-1)}(v) + \mathbf{A}^{(\ell)} \cdot \text{aggr} \left(\left\{ \xi_{\mathcal{G}}^{(\ell-1)}(u) \mid u \in \mathcal{N}_{\mathcal{G}}(v) \right\} \right) + \mathbf{b}^{(\ell)} \right),$$

where $\{\cdot\}$ denotes a multiset.

Once the features are computed, we can apply a threshold to produce a classification of nodes. The GNN assigns each node to one of the classes $\{1, \dots, d^{(L)}\}$ based on its final-layer features.

Definition 10 (Classifier induced by a GNN). Let \mathcal{A} be an L -layer GNN and $\mathcal{G} \in \mathfrak{G}_{V,X}$. For a vertex $v \in V$, the predicted class of \mathcal{A} on v , denoted by $\hat{c}(\mathcal{G}, v)$, is

$$\hat{c}(\mathcal{G}, v) := \arg \max_{1 \leq i \leq d^{(L)}} \left(\xi_{\mathcal{G}}^{(L)}(v) \right) [i].$$

2.2 Adversarial Robustness of GNNs

Unlike standard feedforward neural networks, whose features and predictions depend only on the input features; GNN computation depends on both the input features and the structure of the input graph. Consequently, GNN features and predictions may change under two types of perturbations [BG19, HZCM24, MLK25]: (i) *feature perturbations*, where an adversary modifies node features, and (ii) *structural perturbations*, where an adversary inserts or deletes edges. In this work we study adversarial robustness under *structural perturbations only*: given a GNN \mathcal{A} , a featured graph \mathcal{G} , and an admissible perturbation budget, we ask whether the prediction of \mathcal{A} remains unchanged for *every* graph within the admissible perturbation margin around \mathcal{G} .

We formalize admissible perturbations via an *admissible perturbation space of graphs*, following prior work [BG19, HZCM24, MLK25]. Throughout, we restrict to structural perturbations, that is, edge insertions and deletions, while keeping node features fixed.

Definition 11 (Admissible perturbation space of a graph). *Given a graph $\mathcal{G} = \langle V, E, X \rangle$, a set of fragile edges $F \subseteq V \times V$, a global perturbation budget Δ , and a local perturbation budget δ , the admissible perturbation space $\Omega(\mathcal{G}, F, \Delta, \delta)$ of \mathcal{G} with respect to F , Δ , and δ is the set of graphs $\langle V, E', X \rangle$ that satisfy:*

1. $E \setminus F \subseteq E' \subseteq E \cup F$.
2. $|E \setminus E'| + |E' \setminus E| \leq \Delta$.
3. For every $v \in V$, $|\mathcal{N}_{\mathcal{G}}(v) \setminus \mathcal{N}_{\mathcal{G}'}(v)| + |\mathcal{N}_{\mathcal{G}'}(v) \setminus \mathcal{N}_{\mathcal{G}}(v)| \leq \delta$.

The above conditions are equivalent to requiring that \mathcal{G}' can be obtained from \mathcal{G} by converting at most Δ edges from F . Moreover, for every vertex $v \in V$, at most δ of its incident edges are converted. We will also consider the admissible perturbation space without local budget limitations. In this case, we simply write $\Omega(\mathcal{G}, F, \Delta)$.

The choice of the fragile-edge set F captures different scenarios. For example, in the *deletion-only* case, setting $F = E$ allows the adversary to delete existing edges but not insert new ones; if we set $F = (V \times V) \setminus \{(v, v) : v \in V\}$, the adversary may insert or delete any non-self-loop edge.

We now formalize the notion of adversarial robustness for GNNs.

Definition 12 (Adversarial robustness of GNNs). *Let \mathcal{A} be an L -layer GNN, \mathcal{G} a graph, $F \subseteq V \times V$ a set of edges, $\Delta \in \mathbb{N}$ a global budget, and $\delta \in \mathbb{N}$ a local budget. For a class $1 \leq c \leq d^{(L)}$, we define the adversarial robustness of \mathcal{A} with respect to c as follows:*

For a vertex $v \in V$, we say that \mathcal{A} is adversarially robust for v with class c if, for every perturbed graph $\mathcal{G}' \in \Omega(\mathcal{G}, F, \Delta, \delta)$, it holds that $\hat{c}(\mathcal{G}', v) = c$.

Note that the condition in the above definition is equivalent to requiring that, for every $1 \leq c' \neq c \leq d^{(L)}$,

$$\xi_{\mathcal{G}'}^{(L)}(v)[c] \geq \xi_{\mathcal{G}'}^{(L)}(v)[c'].$$

This formulation requires robustness against *every* alternative class $c' \neq c$. These problems are easily seen to be NP-complete even for a fixed GNN and a very simple update model: see the appendix for a precise statement and a proof, which follows along the lines of similar results for feedforward networks [KBD⁺17, SL21].

Definition 13 (Adversarial robustness radius of GNNs). *Let \mathcal{A} be an L -layer GNN, \mathcal{G} a graph, and $F \subseteq V \times V$ a set of edges. For a class $1 \leq c \leq d^{(L)}$, we define the adversarial robustness radius of \mathcal{A} with respect to c as follows:*

For a vertex $v \in V$, the adversarial robustness radius of \mathcal{A} for v with class c is the maximum global budget Δ such that \mathcal{A} is adversarial robust for v with respect to c .

In the body of the paper we focus on the node classification case. The variation for graph classification is similar: see appendix B.

3 Lightweight robustness analysis graph neural networks

We overview our approach to robustness analysis. Consider the following generalization of the robustness verification problem:

Definition 14 (d-radius satisfaction). *Given property \mathcal{Q} a normal graph \mathcal{G} , an incomplete graph \mathcal{H} with the same vertex set and input feature mapping as \mathcal{G} , and a vertex $v \in V$, we say that property \mathcal{Q} is satisfied within radius d of \mathcal{G} at v with respect to \mathcal{H} if there exists a completion \mathcal{G}' of \mathcal{H} with $\text{dist}(\mathcal{G}', \mathcal{G}) \leq \text{dist}(\mathcal{H}, \mathcal{G}) + d$ such that $\langle \mathcal{G}', v \rangle$ satisfies \mathcal{Q} .*

We will also consider the following search problem variant.

Definition 15 (Radius of satisfaction). *Given property \mathcal{Q} a normal graph \mathcal{G} , an incomplete graph \mathcal{H} with the same vertex set V and features X as \mathcal{G} , a vertex $v \in V$, and a maximum budget $d_m \in \mathbb{N}$, the radius of satisfaction of \mathcal{Q} of \mathcal{G} at v with respect to \mathcal{H} is the largest $d \leq d_m$, such that for every completion \mathcal{G}' of \mathcal{H} with $\text{dist}(\mathcal{G}', \mathcal{G}) \leq d$, $\langle \mathcal{G}', v \rangle$ does not satisfy \mathcal{Q} .*

Assuming membership in the property \mathcal{Q} is decidable, we can decide the problems defined above, since a naive algorithm can enumerate completions of \mathcal{H} , and check whether they satisfy \mathcal{Q} and the distance constraint.

Rather than using a naive algorithm, we aim to solve these problems by employing a *partial oracle*.

Definition 16 (Partial oracle). *For a node property \mathcal{Q} , a normal graph \mathcal{G} with the vertex set V and features X , and a vertex $v \in V$, a partial oracle for \mathcal{Q} , \mathcal{G} , and v , denoted by $\mathcal{O}_{\mathcal{Q}, \mathcal{G}, v}$, is a function that receives an incomplete graph $\mathcal{H} \in \mathfrak{H}_{V, X}$ and a budget $d \in \mathbb{N}$ as input, and which outputs either **SAT**, **UNSAT**, or **UNKNOWN**, and satisfy the following conditions:*

1. *(Correctness for SAT) If $\mathcal{O}_{\mathcal{Q}, \mathcal{G}, v}(\mathcal{H}, d)$ returns **SAT**, then there exists a completion \mathcal{G}' of \mathcal{H} with $\text{dist}(\mathcal{G}', \mathcal{G}) \leq \text{dist}(\mathcal{H}, \mathcal{G}) + d$ such that $\langle \mathcal{G}', v \rangle$ satisfies \mathcal{Q} .*
2. *(Correctness for UNSAT) If $\mathcal{O}_{\mathcal{Q}, \mathcal{G}, v}(\mathcal{H}, d)$ returns **UNSAT**, then for every completion \mathcal{G}' of \mathcal{H} with $\text{dist}(\mathcal{G}', \mathcal{G}) \leq \text{dist}(\mathcal{H}, \mathcal{G}) + d$, $\langle \mathcal{G}', v \rangle$ does not satisfy \mathcal{Q} .*
3. *(Soundness on normal graphs or zero budget) If \mathcal{H} is normal or $d = 0$, then $\mathcal{O}_{\mathcal{Q}, \mathcal{G}, v}(\mathcal{H}, d)$ never returns **UNKNOWN**.*

We can solve the d radius satisfaction problem by the following depth-first search (DFS) Algorithm 1, which searches through completions of \mathcal{H} for boosting a partial oracle into an exact solution. The search procedure is guided by the partial oracle $\mathcal{O}_{\mathcal{Q}, \mathcal{G}, v}$, that is, if the oracle returns either **SAT** or **UNSAT**, then the search procedure returns from the current branch with **SAT** or **UNSAT** immediately. If the oracle returns **UNKNOWN**, the algorithm converts an unknown edge to either a non-edge or a normal edge and proceeds recursively. The correctness can be established by induction on the number of unknown edges.

Designing a higher-quality oracle can significantly reduce the number of oracle calls compared to the naive approach. However, there is always a trade-off between the quality of the oracle and its cost: an exact oracle can be obtained by exhaustively checking all exponentially many normal graphs, whereas a trivial sloppy oracle may simply return **UNKNOWN** for every non-normal graph.

We will solve the adversarial robustness problem for GNNs via Algorithm 1, using a polynomial time partial oracle. We focus on node classification under an unbounded local budget: no per-vertex constraint on the number of perturbed edges. Once we have obtained a partial oracle for the d -radius satisfaction problem, we could apply it naively to compute the distance for satisfaction, which corresponds to the adversarial robustness radius problem.

We fix an L -layer GNN \mathcal{A} , a graph \mathcal{G} with set of vertices V and feature mapping X , a vertex $v_0 \in V$, a set of fragile edges $F \subseteq V \times V$, a global budget Δ , and a class $1 \leq c \leq d^{(L)}$.

Consider the relaxation of \mathcal{G} with respect to F , which is denoted by $\mathcal{H}_{\mathcal{G}, F}$. Recall that $\mathcal{H}_{\mathcal{G}, F}$ is the incomplete graph obtained by converting all the edges and non-edges in F into unknown edges. By Lemma 2, we have $\text{dist}(\mathcal{H}_{\mathcal{G}, F}, \mathcal{G}) = 0$. We first observe that the admissible perturbation space $\mathfrak{Q}(\mathcal{G}, F, \Delta)$ coincides with the set of completions \mathcal{G}' of $\mathcal{H}_{\mathcal{G}, F}$ satisfying $\text{dist}(\mathcal{G}', \mathcal{G}) \leq \Delta$.

Let $\mathcal{Q}_{\mathcal{A}, c}$ be the node property that holds on node v_0 in \mathcal{G}' when there exist $1 \leq c' \neq c \leq d^{(L)}$ such that

$$\xi_{\mathcal{G}'}^{(L)}(v_0)[c] < \xi_{\mathcal{G}'}^{(L)}(v_0)[c'].$$

Algorithm 1 Algorithm for solving the d radius satisfaction problem.

```

1: procedure CHECK( $\mathcal{Q}, \mathcal{G}, v, \mathcal{H}, d$ )
2:   OracleResult  $\leftarrow \mathcal{O}_{\mathcal{Q}, \mathcal{G}, v}(\mathcal{H}, d)$ 
3:   if OracleResult is SAT then
4:     return SAT
5:   else if OracleResult is UNSAT then
6:     return UNSAT
7:   else
8:     Pick  $e \in E_{\text{Unk}}$ 
9:     if  $e$  is an edge in  $\mathcal{G}$  then
10:        $\mathcal{H}_1 \leftarrow \mathcal{H}$  by converting  $e$  into a normal edge.
11:        $\mathcal{H}_2 \leftarrow \mathcal{H}$  by converting  $e$  into a non-edge.
12:     else
13:        $\mathcal{H}_1 \leftarrow \mathcal{H}$  by converting  $e$  into a non-edge.
14:        $\mathcal{H}_2 \leftarrow \mathcal{H}$  by converting  $e$  into a normal edge.
15:     end if
16:     if (CHECK( $\mathcal{Q}, \mathcal{G}, v, \mathcal{H}_1, d$ ) return SAT) or (CHECK( $\mathcal{Q}, \mathcal{G}, v, \mathcal{H}_2, d - 1$ ) return SAT) then
17:       return SAT
18:     else
19:       return UNSAT
20:     end if
21:   end if
22: end procedure

```

If there exists a perturbed graph $\mathcal{G}' \in \mathfrak{Q}(\mathcal{G}, F, \Delta)$, such that $\langle \mathcal{G}', v_0 \rangle$ satisfies \mathcal{Q} , then \mathcal{A} is not adversarially robust for v_0 with class c . Thus, verifying the *non-adversarial robustness* of \mathcal{A} for v_0 with class c can be reduced to solving the d -radius satisfaction problem as follows:

Does there exist a normal graph $\mathcal{G}' \subseteq \mathcal{H}_{\mathcal{G}, F}$ with $\text{dist}(\mathcal{G}', \mathcal{G}) \leq \Delta$ such that $\langle \mathcal{G}', v \rangle$ satisfies $\mathcal{Q}_{\mathcal{A}, c}$?

We next present a polynomial time partial oracle for the node property $\mathcal{Q}_{\mathcal{A}, c}$. We will describe it for general incomplete graphs \mathcal{H} , not just for $\mathcal{H}_{\mathcal{G}, F}$. The partial oracle consists of two sequential components: a non-robustness tester, and a bound propagator. It returns SAT (resp. UNSAT) if any of the components returns SAT (resp. UNSAT). Otherwise, it returns UNKNOWN.

Non-robustness tester The non-robustness tester evaluates the grounding \mathcal{G}' of \mathcal{H} with respect to \mathcal{G} and returns SAT if the grounding \mathcal{G}' satisfies $\mathcal{Q}_{\mathcal{A}, c}$; otherwise, it returns UNKNOWN. Recall that the grounding is the completion of \mathcal{H} that is closest to \mathcal{G} . By Lemma 1, we have $\text{dist}(\mathcal{G}', \mathcal{G}) = \text{dist}(\mathcal{H}, \mathcal{G}) \leq \text{dist}(\mathcal{H}, \mathcal{G}) + d$ for any $d \in \mathbb{N}$. Therefore, if \mathcal{G}' satisfies $\mathcal{Q}_{\mathcal{A}, c}$, then \mathcal{G}' is a non-robust normal graph within the admissible perturbation space.

Bound propagator For the robustness tester, we abstract the computation of a GNN on an incomplete graph by computing upper and lower bounds for features at each vertex v and each layer ℓ : we denote these by $\bar{\xi}_{\mathcal{H}}^{(\ell)}(v)$ and $\underline{\xi}_{\mathcal{H}}^{(\ell)}(v)$. The bounds are computed in a bottom-up manner, with the correctness condition being that for every completion \mathcal{G}' of \mathcal{H} , it holds that

$$\underline{\xi}_{\mathcal{H}}^{(\ell)}(v) \leq \xi_{\mathcal{G}'}^{(\ell)}(v) \leq \bar{\xi}_{\mathcal{H}}^{(\ell)}(v).$$

Note that vector comparisons are performed entrywise. After computing the over-approximated bounds, we check that, for every $1 \leq c' \neq c \leq d^{(L)}$,

$$\bar{\xi}_{\mathcal{H}}^{(L)}(v_0)[c] < \underline{\xi}_{\mathcal{H}}^{(L)}(v_0)[c'].$$

If this condition holds, then for every completion \mathcal{G}' of \mathcal{H} , we have

$$\xi_{\mathcal{G}'}^{(L)}(v_0)[c] \leq \bar{\xi}_{\mathcal{H}}^{(L)}(v_0)[c] < \underline{\xi}_{\mathcal{H}}^{(L)}(v_0)[c'] \leq \xi_{\mathcal{G}'}^{(L)}(v_0)[c'],$$

which implies that $\langle \mathcal{G}', v_0 \rangle$ do not satisfy $\mathcal{Q}_{\mathcal{A},c}$.

We need some auxiliary functions for capturing bound propagation for matrix multiplication and aggregation functions. First, for $\mathbf{A} \in \mathbb{R}^{m \times n}$ and $\bar{\mathbf{v}}, \underline{\mathbf{v}} \in \mathbb{R}^n$, we define

$$\overline{\text{relax}}(\mathbf{A}, \bar{\mathbf{v}}, \underline{\mathbf{v}}) := \mathbf{A}^+ \cdot \bar{\mathbf{v}} + \mathbf{A}^- \cdot \underline{\mathbf{v}} \quad \text{and} \quad \underline{\text{relax}}(\mathbf{A}, \bar{\mathbf{v}}, \underline{\mathbf{v}}) := \mathbf{A}^+ \cdot \underline{\mathbf{v}} + \mathbf{A}^- \cdot \bar{\mathbf{v}},$$

where matrices $\mathbf{A}^+, \mathbf{A}^- \in \mathbb{R}^{m \times n}$ are defined entrywise by

$$\mathbf{A}^+ := \max(\mathbf{A}, 0) \quad \text{and} \quad \mathbf{A}^- := \min(\mathbf{A}, 0).$$

These are lower and upper approximations for matrix multiplication, as captured in the following lemma:

Lemma 3. *For every $\mathbf{A} \in \mathbb{R}^{m \times n}$ and $\bar{\mathbf{v}}, \mathbf{v}, \underline{\mathbf{v}} \in \mathbb{R}^n$ with $\underline{\mathbf{v}} \leq \mathbf{v} \leq \bar{\mathbf{v}}$, it holds that*

$$\underline{\text{relax}}(\mathbf{A}, \bar{\mathbf{v}}, \underline{\mathbf{v}}) \leq \mathbf{A} \cdot \mathbf{v} \leq \overline{\text{relax}}(\mathbf{A}, \bar{\mathbf{v}}, \underline{\mathbf{v}}).$$

Next, we define upper and lower approximations for the aggregation functions.

Definition 17. *Let S_1 and S_2 be multisets of reals.*

- For **sum** aggregation, we define

$$\begin{aligned} \overline{\text{sum}}(S_1, S_2) &:= \sum_{s \in S_1} s + \sum_{s \in S_2} \max(s, 0) \\ \underline{\text{sum}}(S_1, S_2) &:= \sum_{s \in S_1} s + \sum_{s \in S_2} \min(s, 0). \end{aligned}$$

- For **max** aggregation, we define $\overline{\text{max}}(S_1, S_2) := \max(S_1 \cup S_2)$. If $S_1 = \emptyset$, then we set $\underline{\text{max}}(S_1, S_2) := \min(0, \min(S_2))$; otherwise $\underline{\text{max}}(S_1, S_2) := \max(S_1)$. For convention, we let $\max(\emptyset) = 0$.
- For **mean** aggregation, let $s_1, \dots, s_{|S_2|}$ be the elements of S_2 arranged in descending order. We define

$$\begin{aligned} \overline{\text{mean}}(S_1, S_2) &:= \max_{1 \leq i \leq |S_2|} \left(\left(\sum_{s \in S_1} s + \sum_{1 \leq j \leq i} s_j \right) / (|S_1| + i) \right) \\ \underline{\text{mean}}(S_1, S_2) &:= \max_{1 \leq i \leq |S_2|} \left(\left(\sum_{s \in S_1} s + \sum_{|S_2|-i \leq j \leq |S_2|} s_j \right) / (|S_1| + i) \right). \end{aligned}$$

We are now ready to define the over-approximated upper and lower bounds for GNN computation.

For $\ell = 0$, $\bar{\xi}_{\mathcal{H}}^{(0)}(v) = \underline{\xi}_{\mathcal{H}}^{(0)}(v) := X(v)$. For $1 \leq \ell \leq L$ and $v \in V$,

$$\begin{aligned} \bar{\xi}_{\mathcal{H}}^{(\ell)}(v) &:= \text{ReLU} \left(\overline{\text{relax}} \left(\mathbf{C}^{(\ell)}, \bar{\xi}_{\mathcal{H}}^{(\ell-1)}(v), \underline{\xi}_{\mathcal{H}}^{(\ell-1)}(v) \right) + \overline{\text{relax}} \left(\mathbf{A}^{(\ell)}, \bar{\mathbf{s}}, \underline{\mathbf{s}} \right) + \mathbf{b}^{(\ell)} \right) \\ \underline{\xi}_{\mathcal{H}}^{(\ell)}(v) &:= \text{ReLU} \left(\underline{\text{relax}} \left(\mathbf{C}^{(\ell)}, \bar{\xi}_{\mathcal{H}}^{(\ell-1)}(v), \underline{\xi}_{\mathcal{H}}^{(\ell-1)}(v) \right) + \underline{\text{relax}} \left(\mathbf{A}^{(\ell)}, \bar{\mathbf{s}}, \underline{\mathbf{s}} \right) + \mathbf{b}^{(\ell)} \right), \end{aligned}$$

where

$$\bar{\mathbf{s}} := \overline{\text{aggr}} \left(\bar{S}^{\text{Norm}}, \bar{S}^{\text{Unk}} \right) \quad \text{and} \quad \underline{\mathbf{s}} := \underline{\text{aggr}} \left(\underline{S}^{\text{Norm}}, \underline{S}^{\text{Unk}} \right),$$

with $\bar{S}^{\text{Norm}} := \left\{ \bar{\xi}_{\mathcal{H}}^{(\ell-1)}(u) \mid u \in \mathcal{N}_{\mathcal{H}}^{\text{Norm}}(v) \right\}$ and $\underline{S}^{\text{Norm}}, \bar{S}^{\text{Unk}}, \underline{S}^{\text{Unk}}$ defined analogously.

The upper and lower bounds are computed in a bottom-up manner. For each layer ℓ and each vertex v :

- With **sum** and **max** aggregations, the bounds can be obtained in time linear in the number of neighbors of v .
- With **mean** aggregation, the bounds are computed by first sorting the neighbor bounds from the previous layer, with this sorting step dominating the overall cost.

Combining these results, the total time complexity is $O(L|V|^2)$ for **sum** and **max**, and $O(L|V|^2 \log |V|)$ for **mean**, where $|V|$ denotes the number of vertices in the graph and L denotes the number of GNN layers.

The correctness of the over-approximated upper and lower bounds can be proven inductively.

Lemma 4. *For every completion \mathcal{G}' of \mathcal{H} , $0 \leq \ell \leq L$, and vertex $v \in V$, it holds that*

$$\underline{\xi}_{\mathcal{H}}^{(\ell)}(v) \leq \xi_{\mathcal{G}'}^{(\ell)}(v) \leq \bar{\xi}_{\mathcal{H}}^{(\ell)}(v).$$

4 Optimization

We discuss several optimizations of the naïve algorithm. Some are based on the architecture of GNNs, while others leverage the structure of the input graph.

Incremental Computation for the Partial Oracle Recall that the partial oracle for adversarial robustness of GNNs, defined previously consists of two components: the non-robustness tester and the bound propagator. Both components compute features or their over-approximated bounds in a bottom-up manner, where each value depends on the features or bounds of its neighbors from the previous layer. This process involves $|V| \cdot L$ computations in total.

The main idea for speeding up the computation for the partial oracle is therefore to cache the features and bounds of all vertices at all layers for the current recursive call. During recursion, we only update values for the vertices affected by the edge operation, while reusing previously stored results for unaffected vertices. When returning from a recursive call, the cache of the modified features and bounds is restored to its prior state.

For example, suppose we have computed the features and bounds for the current graph, and then convert the edge (v, u) in the graph, either from non-edge to edge, or vice versa.

- (Layer 0.) The features are given by X , which are independent of the graph structure, so no updates are required.
- (Layer 1.) Only v and u need to update their features and over-approximated bounds.
- (Layer 2.) In addition to v and u , their neighbors $\mathcal{N}_\mathcal{H}^{\text{Norm}}(v) \cup \mathcal{N}_\mathcal{H}^{\text{Unk}}(v)$ and $\mathcal{N}_\mathcal{H}^{\text{Norm}}(u) \cup \mathcal{N}_\mathcal{H}^{\text{Unk}}(u)$ must also be updated.
- (Layer ℓ .) At layer ℓ , we update vertices which are updated in layer $\ell - 1$ and their neighbors. In general, we update all vertices within distance at most $\ell - 1$ from either v or u .

Furthermore if at any layer we detect that a vertex w 's feature or bound does not change, then its neighbors need not be updated in the next layer.

We can further reduce the number of updates by tracking the distance between a vertex w and the target vertex v_0 . Recall that the outcome of node classification depends on the feature of v_0 at the last layer L . For a vertex w with distance d to v_0 , for any $\ell > L - d$, the ℓ^{th} layer feature of w will *not* affect the final feature of v_0 . Therefore, at the beginning of updating the ℓ^{th} , we can prune nodes that are farther than $L - \ell$ from v_0 . These pruning avoids unnecessary recomputation and further improves efficiency.

Reordering Operations In the computation of vertex features, aggregation over neighbors is followed by a matrix multiplication. For GNNs with **sum** or **mean** aggregations, the order of these operations can be exchanged, that is

$$\begin{aligned} \mathbf{A}^{(\ell)} \cdot \mathbf{sum} \left(\left\{ \xi_{\mathcal{G}}^{(\ell-1)}(u) \mid u \in \mathcal{N}_{\mathcal{G}}(v) \right\} \right) &= \mathbf{sum} \left(\left\{ \mathbf{A}^{(\ell)} \cdot \xi_{\mathcal{G}}^{(\ell-1)}(u) \mid u \in \mathcal{N}_{\mathcal{G}}(v) \right\} \right) \\ \mathbf{A}^{(\ell)} \cdot \mathbf{mean} \left(\left\{ \xi_{\mathcal{G}}^{(\ell-1)}(u) \mid u \in \mathcal{N}_{\mathcal{G}}(v) \right\} \right) &= \mathbf{mean} \left(\left\{ \mathbf{A}^{(\ell)} \cdot \xi_{\mathcal{G}}^{(\ell-1)}(u) \mid u \in \mathcal{N}_{\mathcal{G}}(v) \right\} \right). \end{aligned}$$

This reordering is trivial for non-robustness tester. However, it improves efficiency of bound propagator by allowing us to shrink the over-approximated upper and lower bounds. Intuitively, over-approximated upper bounds for **aggr** are computed for each entry by selecting certain neighbors. If we perform aggregation first, each entry is chosen independently, and the resulting bounds are later obtained through matrix multiplication. But we know that once a neighbor is chosen for the i^{th} entry, the corresponding j^{th} entry is also determined. By performing the matrix multiplication first, we preserve this dependency between entries, which leads to tighter bounds.

Formally, let $\mathbf{A} \in \mathbb{R}^{m \times n}$, and let $\bar{S}_1 = \{\bar{s}_{1,1}, \dots, \bar{s}_{1,k_1}\}$, $S_1 = \{s_{1,1}, \dots, s_{1,k_1}\}$, $\bar{S}_2 = \{\bar{s}_{2,1}, \dots, \bar{s}_{2,k_2}\}$, and $S_2 = \{s_{2,1}, \dots, s_{2,k_2}\}$ be multisets of real vectors in \mathbb{R}^n . Then we have the bound relaxation for

the usual order:

$$\begin{aligned}
& \overline{\text{relax}}(\mathbf{A}, \overline{\text{sum}}(\bar{S}_1, \bar{S}_2), \text{sum}(S_1, S_2)) \\
&= \overline{\text{relax}}\left(\mathbf{A}, \sum_{1 \leq i \leq k_1} \bar{s}_{1,i} + \sum_{1 \leq i \leq k_2} \max(\bar{s}_{2,i}, 0), \sum_{1 \leq i \leq k_1} s_{1,i} + \sum_{1 \leq i \leq k_2} \min(s_{2,i}, 0)\right) \\
&= \sum_{1 \leq i \leq k_1} (\mathbf{A}^+ \cdot \bar{s}_{1,i} + \mathbf{A}^- \cdot s_{1,i}) + \sum_{1 \leq i \leq k_2} (\mathbf{A}^+ \cdot \max(\bar{s}_{2,i}, 0) + \mathbf{A}^- \cdot \min(s_{2,i}, 0)).
\end{aligned}$$

On the other hand, if we apply matrix multiplication before aggregation, we obtain

$$\begin{aligned}
& \overline{\text{sum}}(\{\overline{\text{relax}}(\bar{s}_{1,i}, s_{1,i}) \mid 1 \leq i \leq k_1\}, \{\overline{\text{relax}}(\bar{s}_{2,i}, s_{2,i}) \mid 1 \leq i \leq k_2\}) \\
&= \sum_{1 \leq i \leq k_1} (\mathbf{A}^+ \cdot \bar{s}_{1,i} + \mathbf{A}^- \cdot s_{1,i}) + \sum_{1 \leq i \leq k_2} \max((\mathbf{A}^+ \cdot \bar{s}_{2,i} + \mathbf{A}^- \cdot s_{2,i}), 0).
\end{aligned}$$

Since \mathbf{A}^+ are positive, and \mathbf{A}^- are negative entrywise, we have that for each $1 \leq i \leq m$:

$$\begin{aligned}
\mathbf{A}^+ \cdot \max(\bar{s}_{2,i}, 0) + \mathbf{A}^- \cdot \min(s_{2,i}, 0) &\geq \mathbf{A}^+ \cdot \bar{s}_{2,i} + \mathbf{A}^- \cdot s_{2,i} \\
\mathbf{A}^+ \cdot \max(\bar{s}_{2,i}, 0) + \mathbf{A}^- \cdot \min(s_{2,i}, 0) &\geq 0.
\end{aligned}$$

Therefore, the reordered computation yields a tighter (smaller) upper bound.

The arguments for the lower bound and for **mean** aggregation are analogous.

We can further reduce the number of computations by incorporating operator reordering and incremental computation, caching the feature and bounds at each layer before computing the next layer. For example, suppose that at layer ℓ , we update only a vertex v . According to the setup of incremental computation, we then need to update all k neighbors of v at layer $\ell + 1$. In the normal computation order, we would perform aggregation and matrix multiplication k times. However, with operator reordering, we can first compute the matrix multiplication between the coefficients and the updated feature of v at layer ℓ ; then, in the next step, we only need to apply aggregation k times, thereby saving $k - 1$ matrix multiplications.

Bound Tightening of Aggregation Functions Using Budgets The bound propagator described earlier computes over-approximated bounds for *all* completions of the input incomplete graph \mathcal{H} . However, when the perturbation budget is limited, these bounds can be further tightened by explicitly incorporating the budget constraint.

For example, consider a GNN with **sum** aggregation, where the global perturbation budget is 2. Suppose vertex v has 5 unknown incoming edges, all of which are normal edges in the target graph \mathcal{G} . Under the naive propagation rule given earlier, the lower bound is obtained by summing all negative lower bounds from these 5 neighbors. If all neighbor features are positive, this procedure yields a trivial lower bound of 0. Now note that, because the budget is 2, at least 3 of the 5 unknown edges must remain present. Therefore, instead of discarding all 5 contributions, the lower bound should be given by the sum of the 3 smallest neighbor features. Since all features are positive, this bound is strictly greater than 0. This example shows how budget constraints can significantly tighten the propagated bounds.

The budget-aware bound tightening for **sum** aggregation was established in [HZCM24]. The corresponding results for **max** and **mean** aggregations were shown by [MLK25].

Note that, unlike reordering operations, bound shrinking can be achieved without additional overhead. For bound tightening of aggregation functions using budgets, however, extra computation (e.g. sorting) is required to determine the bounds based on the budget, compared to the naïve algorithms. Although the tighter bounds may reduce the number of oracle calls, the computation time per oracle call increases. As a result, there is no guarantee of a decrease in the overall runtime.

Graph Structure Heuristics for Edge Picking in the High-level algorithm Thus far we have focused on optimizations within the lightweight oracles. In the high-level Algorithm 1 that uses these oracles, graph structure can be exploited to accelerate termination. The high-level algorithm is order-sensitive: the amount of branch pruning depends heavily on which unknown edge is selected next (cf. line 8). We outline several practical heuristics; the high-level idea is to pick the edge whose resolution is expected to affect most amount of features.

- For node classification, for the target vertex v_0 , prioritize unknown edges that are *closest* to v_0 . If an edge is at distance r from v_0 , it can influence the feature of v_0 only starting from layer $L - r$, where L is the GNN depth. Choosing small- r edges typically maximizes the impact on the final-layer feature of v_0 and tends to minimize the connected region that contains v_0 .
- For node classification, if the incomplete graph \mathcal{H} decomposes into several disconnected components, restrict edge choices to the component that contains the target vertex v_0 . Edges outside this component cannot affect the feature of v_0 and only enlarge the search space.
- After picking the unknown edge e , we recursively consider two subproblems with inputs \mathcal{H}_1 and \mathcal{H}_2 by setting e to match its status in the target graph \mathcal{G} for \mathcal{H}_1 , and to the opposite status for \mathcal{H}_2 . In general, the order in which we perform the recursive calls for \mathcal{H}_1 and \mathcal{H}_2 does not affect the correctness of the algorithm, since we later consider the disjunction of results of both recursive calls (cf. line 16). However, the order does affect the runtime of the algorithm, because we can terminate early if the first call returns. Our strategy is to explore \mathcal{H}_2 first, since this branch immediately consumes one unit of budget, yielding a smaller search space. Intuitively, it is also more likely to change the features than \mathcal{H}_1 branch (the one consistent with \mathcal{G}).

Edge inference for local budgets The previous optimization exploits the limited *global* budget. In the case of *local* budgets, we can further infer the status of unknown edges whenever a vertex exhausts its local budget.

Consider the following example. Suppose vertex v has 5 unknown incoming edges, all of which are normal edges in the target graph \mathcal{G} , and its local budget is 2. If, after some recursive calls, two of these unknown edges have already been converted into non-edges, then the local budget of v is exhausted. Consequently, all remaining unknown edges incident to v must be normal edges; otherwise, the resulting graph would not belong to the admissible perturbation space. This inference reduces the number of unknown edges, and hence shrinks the search space for Algorithm 1.

For undirected input graphs, this reasoning further tightens the over-approximated bounds of neighboring vertices, since an inferred edge is shared by both endpoints.

In practice, this inference procedure can be applied at the beginning of each recursive call, thereby propagating the consequences of local budget constraints throughout the graph.

5 Experiments

Implementation of ROBLIGHT and Set up Our method is implemented as ROBLIGHT, which supports GNN robustness problems with a variety of aggregation functions (**sum**, **max**, and **mean**) for both node classification and graph classification; for both directed and undirected graphs; and for both deletion-only as well as deletion and insertion perturbations. ROBLIGHT is implemented in C, and all experiments were conducted using the version compiled with GCC 11.4. Experiments were performed on a cluster with Intel Xeon Platinum 8268 CPU @ 2.90GHz with AVX2 support enabled running CentOS 8. Each instance was solved using a single thread with 8GB of RAM. The time limit was set to 300s for node classification instances and 600s for graph classification instances.

Datasets and Models We evaluate the performance of ROBLIGHT on GNN models with various numbers of layers and aggregation functions, built and trained using PyG (PyTorch Geometric) 2.6 [FL19], on the following benchmarks: Cora, CiteSeer [SNB⁺08, YSX⁺23], Cornell, Texas, and Wisconsin [PWC⁺20] for node classification, and MUTAG and ENZYMES [MKB⁺20] for graph classification. Note that Cornell, Texas, and Wisconsin are different from the citation-based benchmarks in that they are *heterophilic*: the existence of an edge between two nodes is not tightly connected to the node labels. We summarize the information on benchmarks in Table 1.

All models are trained for 1000 epochs with a learning rate of 0.001 and a weight decay of 5×10^{-5} . For node datasets, we randomly select 30% of the nodes as the training set, 20% as the validation set, and the remaining 50% as the test set. For graph datasets, we use 80%, 10%, and 10% of the graphs for training, validation, and testing, respectively. The dimensions of hidden layers are set to 32 for node classification and 16 for graph classification. We conduct experiments on directed graphs with deletion-only perturbations for node classification; that is, the set of fragile edges F corresponds to the set of edges of the input graph. For graph classification, we perform both deletion and insertion

perturbations on undirected graphs; that is, the set of fragile edges F includes all edges excluding self-loops.

Recall that the condition of the robustness of a vertex v with respect to the class c is that, for every $1 \leq c' \neq c \leq d^{(L)}$, $\xi_{G'}^{(L)}(v)[c] \geq \xi_{G'}^{(L)}(v)[c']$. We also consider *weak robustness*, in which we only consider perturbations to one fixed target class c' . In our experiments, we set c to be the predicted class by the GNN and $c' = (c \bmod d^{(L)}) + 1$.

Table 1: Information for benchmarks, where *Deg* denotes the average incoming degree of vertices. For graph datasets, *#Vertices* and *#Edges* represent the average number of vertices and edges per graph, respectively.

Dataset	#Vertices	#Edges	Deg	#features	#classes	Dataset	#Graphs	#Vertices	#Edges	Deg	#features	#classes
Cora	2,708	5,429	2.00	1,433	6	MUTAG	188	17.9	39.6	2.21	7	2
CiteSeer	3,312	4,715	1.42	3,70	6	ENZYMES	600	32.6	124.3	3.81	3	6
Cornell	183	298	1.63	1,703	5							
Texas	183	325	1.78	1,703	5							
Wisconsin	251	515	2.05	1,703	5							

Baselines We compare our ROBLIGHT with the most recent available exact tools for GNN robustness checking, SCIP-MPNN [HZCM24] and GNNEV [MLK25], both of which are based on translating the robustness problem into mixed-integer programming (MIP). SCIP-MPNN implements a solver for the weaker version of the GNN robustness problem, supporting node classification for directed graphs with deletion-only perturbations, and graph classification for undirected graphs with both deletion and insertion perturbations; both use **sum** aggregation only. It relies on the open-source MIP solver SCIP [BBC⁺23]. In our experiments, we run SCIP-MPNN using the SCIPsbt setting for node classification and the SCIPabt setting for graph classification. Note that SCIP-MPNN also provides options to solve the MIP instance with the commercial MIP solver Gurobi [Gur24]. However, this implementation is buggy, as mentioned in Appendix B.2 of [HZCM24], and can incorrectly report a feasible instance as infeasible. For consistency, we do not run SCIP-MPNN with Gurobi. GNNEV implements a solver for the GNN robustness problem for node classification on directed graphs with both deletion and insertion perturbation, supporting aggregation functions **sum**, **max**, and **mean**, relying on the commercial MIP solver Gurobi [Gur24]. We run GNNEV with incremental solving enabled.

End to end performance on node classification We first looked to answer the question of how our lightweight solve-based methods compares to the state of the art on standard node classification benchmarks, focusing on the Cora, CiteSeer, Cornell, Texas, and Wisconsin datasets. The number of GNN layers is set to 4, noting that no prior tool has shown consistent performance passed 3 layers. We apply the analysis on each vertex with budgets 1, 2, 5, and 10. We summarize the results on weak robustness for the **sum** aggregation as well as the results on general robustness for the **sum**, **max**, and **mean** aggregations in Table 2, where we sum the number of instances with different budgets. For the shifted geometric mean, we set the shiftb to 10. For the full results for each distinguished budget, see appendix E.1. Figure 1 gives a different view, showing how many instances for each budget can be completed as time increases.

Takeaways The first conclusion is that ROBLIGHT outperforms the baselines by more than an order of magnitude for every set up. In particular, it shows that it can handle 4 layer GNNs, which were beyond the scope of the prior art. In the case of larger budgets, the competitors cannot complete a significant portion of the instances – note that we are showing the average time only for completed instances. For Citeseer, the gap in performance is smaller, related to the fact that Citeseer has a much simpler structure, with average in-degree 1.4 vs. 2 for Cora.

In our algorithm we are also doing constraint-solving. Our advantage is that we are using the structure of the GNN – in each call to our partial oracle and in the optimizations (e.g. caching) of the high-level algorithm. This structure is not transparent to a constraint solver like Gurobi.

For MIP-based solvers, robust instances are easier than non-robust ones, roughly corresponding to unsat vs. sat. For ROBLIGHT, non-robust instances are easier, since on non-robust instances our naïve counterexample finder turns out to be sufficient.

To fairly compare weak robustness and general robustness, we summarize the runtime of instances that are both weakly and generally robust (or non-robust) with budget 10 in Table 3. For instances that are both weakly and generally robust, the runtime increases for both ROBLIGHT and GNNEV, as expected. However, for non-robust instances, compared with GNNEV, whose runtime remains roughly the same, the runtime for general robustness decreases significantly for ROBLIGHT. This is again because our lightweight non-robust tester can quickly find counterexamples.

In terms of the impact of the aggregation function, we see that max is the hardest for ROBLIGHT, and this is because we cannot apply the re-ordering optimization, Bound tightening for max is more effective for ROBLIGHT, as well as for the baseline: but we find that optimizations like re-ordering have larger impact than improvements in bounded tightening.

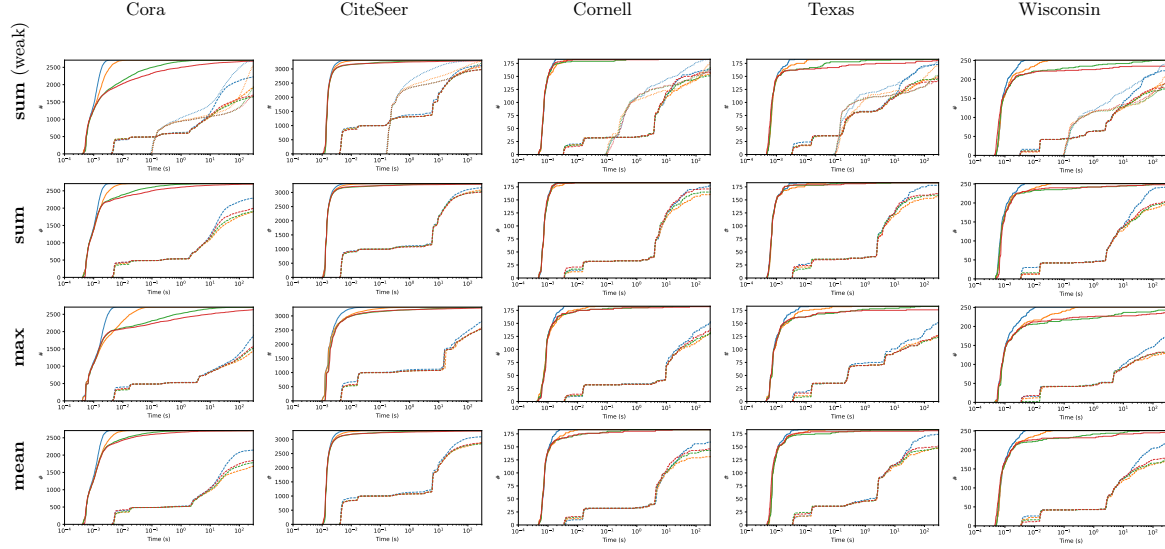
Table 2: Comparison results of ROBLIGHT, GNNEV, and SCIP-MPNN for weak and general robustness on the Cora, CiteSeer, Cornell, Texas, and Wisconsin datasets with various aggregation functions. Note that SCIP-MPNN only implements weak robustness for **sum** aggregation. t_a denotes the average runtime, and t_g denotes the shifted geometric mean of the runtime.

		ROBLIGHT				GNNEV				SCIP-MPNN				
		All instances		Robust instances		All instances		Robust instances		All instances		Robust instances		
		#Instances	#Solved	$t_a(s)$	$t_g(s)$	#Solved	$t_a(s)$	$t_g(s)$	#Solved	$t_a(s)$	$t_g(s)$	#Solved	$t_a(s)$	$t_g(s)$
sum (Weak)	Cora	10,832	10,804	0.50	0.17	9,127	0.54	0.19	7,509	27.13	11.55	6,101	27.36	10.57
	CiteSeer	13,248	13,221	0.21	0.06	11,968	0.23	0.06	12,193	14.70	7.58	10,936	13.77	6.73
	Cornell	732	732	0.01	0.01	416	0.02	0.01	627	15.68	8.37	331	16.46	7.36
	Texas	732	730	0.99	0.23	601	0.91	0.16	611	14.21	6.19	494	9.28	3.95
	Wisconsin	1,004	988	0.60	0.21	836	0.70	0.24	768	18.26	8.92	626	15.62	7.11
sum	Cora	10,832	10,822	0.30	0.09	6,821	0.38	0.12	8,122	23.27	11.11	4,741	17.98	7.17
	CiteSeer	13,248	13,225	0.13	0.04	10,352	0.16	0.06	12,367	15.20	8.09	9,439	13.33	6.34
	Cornell	732	732	0.01	0.01	338	0.01	0.01	675	14.39	8.54	292	15.18	6.76
	Texas	732	732	0.02	0.01	360	0.03	0.03	655	10.42	6.09	273	5.96	3.17
	Wisconsin	1,004	1,001	0.67	0.20	693	0.89	0.25	853	22.11	10.58	547	14.81	6.57
max	Cora	10,832	10,754	1.06	0.35	7,040	1.42	0.47	7,092	93.64	29.53	4,394	55.68	13.75
	CiteSeer	13,248	13,201	0.41	0.12	10,442	0.49	0.14	11,020	71.44	19.23	8,512	45.48	12.38
	Cornell	732	731	0.13	0.06	400	0.23	0.10	559	41.00	18.09	267	27.93	9.98
	Texas	732	725	0.28	0.12	575	0.34	0.14	551	48.44	11.32	433	27.05	5.36
	Wisconsin	1,004	982	1.80	0.44	742	2.12	0.51	621	77.87	17.24	471	52.91	9.97
mean	Cora	10,832	10,830	0.16	0.04	6,871	0.20	0.05	7,473	24.00	12.05	4,235	16.89	7.12
	CiteSeer	13,248	13,232	0.12	0.04	10,373	0.14	0.05	11,708	13.90	7.62	8,887	11.97	5.87
	Cornell	732	732	0.04	0.03	448	0.05	0.04	579	13.96	8.16	311	12.01	6.00
	Texas	732	730	0.22	0.07	451	0.36	0.10	624	14.67	7.04	343	11.29	4.51
	Wisconsin	1,004	999	0.46	0.19	656	0.69	0.27	741	20.96	9.86	439	13.86	5.71

Table 3: Detailed comparison results of ROBLIGHT and GNNEV for weak and general robustness on the Cora, CiteSeer, Cornell, Texas, and Wisconsin datasets with **sum** aggregation for global and local budget 10.

		ROBLIGHT				GNNEV			
		Robust instances		Non-robust instances		Robust instances		Non-robust instances	
		$t_a(s)$	$t_g(s)$	$t_a(s)$	$t_g(s)$	$t_a(s)$	$t_g(s)$	$t_a(s)$	$t_g(s)$
sum (Weak)	Cora	0.75	0.29	0.82	0.18	6.31	2.89	22.02	15.02
	CiteSeer	0.15	0.07	0.04	0.03	7.63	4.19	22.84	17.64
	Cornell	0.01	0.01	0.01	0.01	13.34	5.42	12.73	9.13
	Texas	0.03	0.03	4.41	1.82	0.93	0.67	13.28	12.08
	Wisconsin	0.17	0.11	0.05	0.05	6.08	3.55	30.86	20.24
sum	Cora	1.71	0.50	0.12	0.04	10.44	3.49	25.01	15.95
	CiteSeer	0.26	0.10	0.01	0.01	12.90	5.35	26.55	18.45
	Cornell	0.01	0.01	0.01	0.01	8.62	4.06	11.17	9.04
	Texas	0.05	0.04	0.01	0.01	1.09	0.95	19.19	13.58
	Wisconsin	0.50	0.23	0.01	0.01	8.80	4.10	30.47	19.09

Fig. 1: The number of instances solved by each tool plotted against runtime under different aggregations and budgets. The solid line denotes ROBLIGHT, the dashed line denotes GNNEV, and the dotted line denotes SCIP-MPNN. The blue, orange, green, and red lines correspond to budgets of 1, 2, 5, and 10, respectively. Note that the x axis is in logarithmic scale.



Evaluation of optimization strategies Our second experiment evaluates the optimization strategies described in Section 4. Recall that the runtime of Algorithm 1 depends on both the number of recursive calls and the runtime of each call. We introduce the notion of the *exploration ratio* to quantify how these optimization strategies affect the number of recursive calls. Let F denote the set of fragile edges. Since the number of recursive calls grows exponentially with $|F|$, we define the exploration ratio α to be such that $2^{\alpha \cdot (|F|+1)}$ is the number of recursive calls. That is, the exploration ratio is defined as the logarithm of the number of recursive calls divided by $(|F|+1)$. In the worst case, Algorithm 1 explores all possible $2^{|F|}$ graphs, resulting in $2^{|F|+1} - 1$ recursive calls, which implies an exploration ratio close to 1.

We conducted experiments on several variants of ROBLIGHT that exclude the optimizations described in Section 4. The experiments were performed on the Cora and CiteSeer datasets using 4-layer GNNs with different aggregation functions, with both global and local budgets set to 10. The results are summarized in Table 4, where N/A indicates that the strategy is not applicable in this case. For a fair comparison, we only report instances that solved by all variants. Therefore the average runtime for ROBLIGHT is different from previous experiments. Figure 2 provides a different view, showing how many recursive calls ROBLIGHT and ROBLIGHT without optimization strategies need to solve the instances.

Takeaways The results show that the overall improvement exceeds an order of magnitude. For incremental computation, the exploration ratio remains the same while the average runtime per call decreases, which meets our expectation, since incremental computation only accelerates the oracle’s computation without altering its outcome, thereby producing the same computational path for ROBLIGHT. For operator reordering, the average runtime per call decrease as expected. The average exploration ratio also decreases in this case since we incorporating operator reordering and incremental computation. For bound tightening with budgets, the overall runtime remains roughly the same or slightly increases; this may be because the benefit from shrinking is limited, as indicated by the exploration ratio remaining nearly unchanged. Finally, for heuristic edge picking, the exploration ratio decreases as expected, but the average runtime per call increases because ROBLIGHT must maintain and compute information about the k -hop neighbors in the current graph, which introduces additional computational overhead.

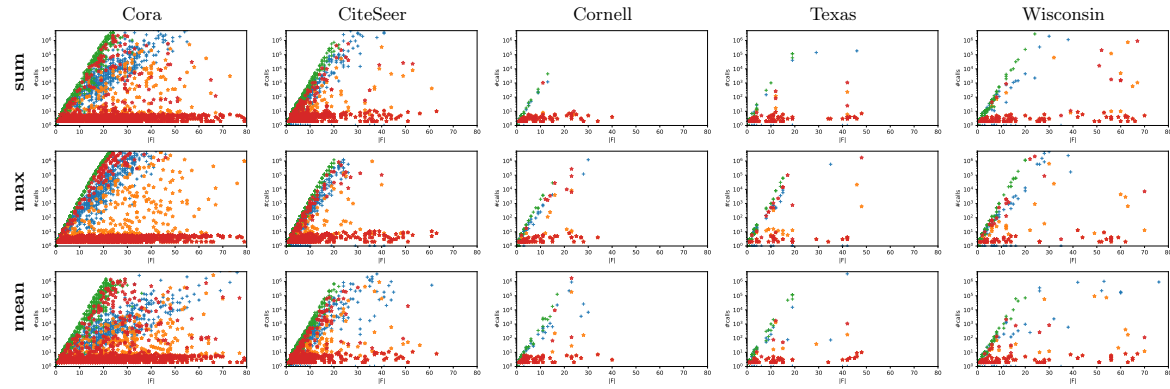
For the non-robust instances, most points lie near the bottom of the figure in Fig 2, regardless of the optimizations applied to ROBLIGHT. This is because most non-robust instances can be quickly identified by our lightweight non-robust tester. For the robust instances, they form a clear line in the diagram, which indicates that the exploration ratio is quite stable across different quantities of fragile

edges in the same instance. Since the y axis is plotted on a logarithmic scale, the slope of the line corresponds to the exploration ratio α . From Fig 2, we can also observe that the slope for ROBLIGHT is smaller than that for ROBLIGHT without optimization strategies.

Table 4: The detailed comparison results of variants of ROBLIGHT on the Cora and CiteSeer datasets using 4-layer GNNs of varying aggregation function, with both global and local budgets set to 10. t_a denotes the average overall runtime, t_c denotes the average runtime per call, and ER denotes the average exploration ratio. N/A indicates that the strategy is not applicable in this case.

		ROBLIGHT			ROBLIGHT w/o inc. comp.			ROBLIGHT w/o operator reorder			ROBLIGHT w/o bound tightening			ROBLIGHT w/o heuristic picking			ROBLIGHT w/o all		
		t_a (s)	t_c (ms)	ER	t_a (s)	t_c (ms)	ER	t_a (s)	t_c (ms)	ER	t_a (s)	t_c (ms)	ER	t_a (s)	t_c (ms)	ER	t_a (s)	t_c (ms)	ER
sum	Cora	0.007	0.009	0.29	0.025	0.032	0.29	0.075	0.057	0.30	0.007	0.009	0.29	0.260	0.005	0.35	10.174	0.168	0.35
	CiteSeer	0.004	0.015	0.40	0.008	0.031	0.40	0.123	0.288	0.40	0.004	0.014	0.40	0.011	0.006	0.42	1.788	0.807	0.42
	Cornell	0.001	0.067	0.31	0.001	0.077	0.31	0.002	0.114	0.31	0.001	0.076	0.31	0.001	0.026	0.32	0.005	0.131	0.32
	Texas	0.003	0.007	0.30	0.022	0.052	0.30	0.026	0.039	0.30	0.003	0.006	0.30	0.016	0.004	0.33	1.428	0.364	0.33
	Wisconsin	0.001	0.016	0.38	0.004	0.042	0.38	0.006	0.056	0.38	0.001	0.016	0.38	0.055	0.003	0.41	3.558	0.194	0.41
max	Cora	0.097	0.035	0.33	0.311	0.116	0.33	N/A	N/A	N/A	0.086	0.031	0.33	1.671	0.021	0.40	16.553	0.130	0.42
	CiteSeer	0.122	0.181	0.41	0.293	0.436	0.41	N/A	N/A	N/A	0.104	0.155	0.41	0.368	0.114	0.45	2.186	0.538	0.46
	Cornell	0.005	0.045	0.37	0.015	0.137	0.37	N/A	N/A	N/A	0.005	0.043	0.37	0.010	0.027	0.43	0.294	0.115	0.44
	Texas	0.006	0.040	0.46	0.017	0.113	0.46	N/A	N/A	N/A	0.006	0.041	0.46	0.150	0.013	0.52	3.851	0.309	0.55
	Wisconsin	0.008	0.048	0.43	0.028	0.169	0.43	N/A	N/A	N/A	0.008	0.047	0.43	0.379	0.017	0.51	4.791	0.162	0.53
mean	Cora	0.002	0.032	0.27	0.006	0.079	0.27	0.043	0.190	0.29	0.002	0.030	0.27	0.170	0.011	0.33	12.485	0.451	0.34
	CiteSeer	0.004	0.032	0.40	0.007	0.065	0.40	0.156	0.565	0.41	0.004	0.032	0.40	0.015	0.015	0.42	2.194	1.218	0.43
	Cornell	0.027	0.023	0.38	0.068	0.056	0.38	0.520	0.204	0.39	0.031	0.020	0.38	0.125	0.016	0.40	3.497	0.319	0.41
	Texas	0.002	0.023	0.35	0.006	0.055	0.35	0.032	0.190	0.35	0.002	0.023	0.35	0.018	0.007	0.40	0.772	0.286	0.40
	Wisconsin	0.001	0.040	0.35	0.002	0.067	0.35	0.006	0.172	0.35	0.001	0.041	0.35	0.006	0.010	0.40	0.403	0.446	0.41

Fig. 2: The number of recursive calls plotted against the number of edges in the set of fragile edges. The blue dots represent the robust instances solved by ROBLIGHT, the orange dots represent the non-robust instances solved by ROBLIGHT, the green dots represent the robust instances solved by ROBLIGHT without any optimization strategies, and the red dots represent the non-robust instances solved by ROBLIGHT without any optimization strategies. Note that the y axis is in logarithmic scale.



Results on robustness radius The third experiment is about the robustness radius, which ROBLIGHT can compute using a variation of the top-level algorithm. We conduct experiments on the Cora and CiteSeer datasets with 4-layer GNNs with varying aggregation functions with timeout 600s. We summarize the results in Table 5.

Note that the true radius in each of these benchmarks is not large: at most 10. Despite this, to our knowledge, *no prior tool can compute the radius exactly*.

Table 5: The results of robust radius of the Cora, CiteSeer, Cornell, Texas, and Wisconsin datasets using 4-layer GNNs of varying aggregation function. TO denotes time out, # denotes the number of instances, and t_a denotes the average overall runtime.

		TO	Robust	$r = 0$	$r = 1$	$r = 2$	$r = 3$	$r = 4$	$r = 5$	$r = 6$	$r = 7$	$r = 8$	$r = 9$	$r = 10$												
		#	# $t_a(s)$																							
sum	Cora	23	1442	2.48	580	0.02	349	0.06	172	2.39	93	1.19	39	2.78	7	6.59	2	12.17	1	11.90	0	N/A	0	N/A	0	N/A
	CiteSeer	31	2428	0.82	493	0.00	199	0.00	85	0.03	39	0.15	12	5.25	9	4.91	9	27.59	3	148.86	2	69.59	0	N/A	2	46.47
	Cornell	0	72	0.00	71	0.00	30	0.00	7	0.04	2	0.03	1	0.74	0	N/A	0	N/A	0	N/A	0	N/A	0	N/A	0	N/A
	Texas	0	77	1.02	68	0.00	25	0.01	9	0.30	3	138.16	0	N/A	1	153.32	0	N/A	0	N/A	0	N/A	0	N/A	0	N/A
	Wisconsin	11	154	3.18	53	0.01	19	0.03	10	0.55	1	5.97	3	193.50	0	N/A	0	N/A	0	N/A	0	N/A	0	N/A	0	N/A
max	Cora	88	1465	9.78	526	1.84	327	0.34	174	2.77	82	29.25	36	74.24	7	146.19	2	90.20	1	158.68	0	N/A	0	N/A	0	N/A
	CiteSeer	50	2474	0.91	507	0.01	152	1.35	84	6.40	25	9.21	13	102.09	4	67.61	2	154.72	1	520.04	0	N/A	0	N/A	0	N/A
	Cornell	1	91	1.07	69	0.01	12	0.06	5	0.32	3	0.21	1	0.09	0	N/A	0	N/A	0	N/A	1	182.61	0	N/A	0	N/A
	Texas	8	135	0.26	26	1.38	9	0.14	5	64.76	0	N/A	0	N/A	0	N/A	0	N/A	0	N/A	0	N/A	0	N/A	0	N/A
	Wisconsin	21	166	9.62	45	1.78	9	0.73	6	4.12	1	0.09	1	27.06	1	17.74	1	574.40	0	N/A	0	N/A	0	N/A	0	N/A
mean	Cora	8	1418	1.16	535	0.00	356	0.05	211	1.61	97	2.03	47	1.64	23	6.07	7	23.36	6	38.40	0	N/A	0	N/A	0	N/A
	CiteSeer	26	2458	0.41	536	0.09	145	0.01	74	0.08	29	0.11	25	5.77	8	21.32	3	64.84	4	168.77	4	1.67	0	N/A	0	N/A
	Cornell	0	99	0.34	51	0.00	16	0.00	7	0.02	5	0.14	3	3.66	1	3.00	0	N/A	0	N/A	1	0.87	0	N/A	0	N/A
	Texas	3	100	0.00	54	0.10	15	0.06	5	0.12	1	0.02	1	0.02	0	N/A	2	0.67	1	35.33	0	N/A	1	1.85	0	N/A
	Wisconsin	8	141	5.24	63	0.00	16	0.19	11	0.63	3	4.05	4	30.45	4	200.58	0	N/A	1	589.55	0	N/A	0	N/A	0	N/A

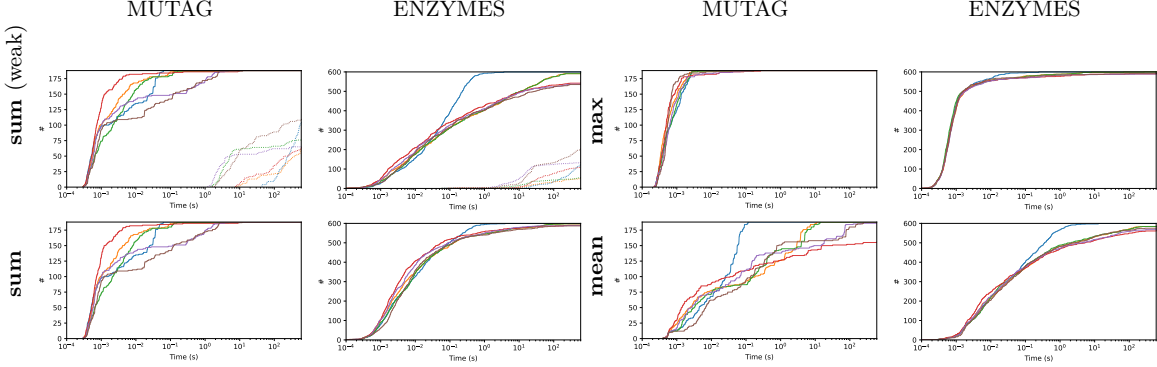
End to end performance on graph classification Finally, we conduct experiments on the MUTAG and ENZYMES datasets, which are undirected and involve graph-level classification instances. In these cases, a final sum pooling operation is applied to obtain a single graph-level output. Details of graph-level robustness and set up for undirected graphs can be found in Appendix B and Appendix C. We consider both deletion and insertion perturbations, as well as a local budget constraint—that is, a local budget smaller than the global one—to demonstrate that ROBLIGHT can effectively handle robustness constraints under various settings. We conduct the experiments with pairs of global and local budget of (1, 1), (2, 1), (2, 2), (5, 1), (5, 2), and (5, 5), respectively. Table 6 summarizes results, and Figure 3 gives a different views, showing how many instances for each budget can be completed as time increases. For the full results for each distinguished budget, see appendix E.2.

Graph classification is more challenging due to this final aggregation layer, we need to keep features and bounds are up to date in each layer for every vertices in the graph. Again, we find that ROBLIGHT can handle up to four layers (excluding the final aggregation layer), surpassing the state of the art. Our method can in fact go beyond four layers, but we did not include a comparison since other solvers timed out on all examples.

Table 6: Comparison results of ROBLIGHT and SCIP-MPNN for weak and general robustness on the MUTAG and ENZYMES datasets with various aggregation functions. Note that SCIP-MPNN only implements weak robustness for **sum** aggregation, thus other entries in the table for SCIP-MPNN are left blank. t_a denotes the average runtime, and t_g denotes the shifted geometric mean of the runtime.

		ROBLIGHT						SCIP-MPNN						
		All instances			Robust instances			All instances			Robust instances			
		#Instances	#Solved	$t_a(s)$	$t_g(s)$	#Solved	$t_a(s)$	$t_g(s)$	#Solved	$t_a(s)$	$t_g(s)$	#Solved	$t_a(s)$	$t_g(s)$
sum	MUTAG (Weak)	1128	1,128	0.11	0.10	58	0.33	0.27	478	128.72	49.44	5	357.92	341.21
	ENZYMES	3600	3,396	6.82	2.37	573	15.38	5.61	672	113.98	50.65	48	188.68	104.27
sum	MUTAG	1128	1,128	0.11	0.10	58	0.33	0.27						
	ENZYMES	3600	3,562	1.51	0.56	166	6.03	2.62						
max	MUTAG	1128	1,128	0.01	0.01	3	0.01	0.01						
	ENZYMES	3600	3,570	0.37	0.11	101	7.80	1.65						
mean	MUTAG	1128	1,093	6.10	2.10	224	2.23	1.92						
	ENZYMES	3600	3,472	5.06	1.68	272	10.15	3.53						

Fig. 3: The number of instances solved by each tool plotted against runtime under different aggregations and budgets. The solid line denotes ROBLIGHT and the dotted line denotes SCIP-MPNN. The blue, orange, green, red, purple, and brown lines correspond to pairs of global and local budget of (1,1), (2,1), (2,2), (5,1), (5,2), and (5,5), respectively. Note that the x axis is in logarithmic scale.



6 Additional related work

A wide range of adversarial attacks can be considered in training machine learning systems, including neural ones: see e.g. [Gün22]. Here we consider the case of attacks on test data at inference time. While our work considers exact methods for determining robustness, there are also incomplete methods [ZAG18, FBZA22], which will sometimes be able to find attacks or infer robustness but sometimes will be inconclusive.

The verification problems we study are straightforwardly decidable since they enumerate over a finite set of inputs. In contrast [SL23, NSST24, BLMT24] consider GNN static analysis problems, quantifying over all inputs.

7 Conclusion

Adversarial robustness problems for discrete settings, such as graph learning, are examples of computationally hard problems, and it is thus natural that prior methods for attacking robustness work on top of solvers for classic hard problems, such as integer programming or SAT. Surprisingly, we show that direct approaches that apply heuristic search on top of lightweight solvers can outperform the state of the art. This indicates that solvers still lack the ability to recognize and exploit structure inherent arising from problems in neural verification, and may prompt investigation in how to adapt general purpose solving tools with these applications in mind.

We note that our work does not consider perturbation both to both the features and the edges. For feature perturbation, the graph neural network robustness problem is quite similar to the robustness problem for standard feedforward neural networks, and so it is natural to proceed via reduction to one of the tools available for analyzing feedforward networks, such as Marabou [KHI⁺19]. We also note that, while our work increases the range of robustness analysis for GNNs, the scalability of such systems is still extremely limited. We know of no tools that report exact analysis beyond GNNs with 4 layers and dimension of the hidden channel in each layer equal to 32.

Bibliography

[AHV95] Serbe Abiteboul, Richard Hull, and Victor Vianu. *Foundations of Databases*. Addison-Wesley, 1995.

[BBC⁺23] Ksenia Bestuzheva, Mathieu Besançon, Wei-Kun Chen, Antonia Chmiela, Tim Donkiewicz, Jasper van Doornmalen, Leon Eifler, Oliver Gaul, Gerald Gamrath, Ambros Gleixner, Leona Gottwald, Christoph Graczyk, Katrin Halbig, Alexander Hoen, Christopher Hojny, Rolf van der Hulst, Thorsten Koch, Marco Lübbecke, Stephen J. Maher, Frederic Matter, Erik Mühmer, Benjamin Müller, Marc E. Pfetsch, Daniel Rehfeldt, Steffan Schlein, Franziska Schlösser, Felipe Serrano, Yuji Shinano, Boro Sofranac, Mark Turner, Stefan Vigerske, Fabian Wegscheider, Philipp Wellner, Dieter Weninger, and Jakob Witzig. Enabling Research through the SCIP Optimization Suite 8.0. *ACM Trans. Math. Softw.*, 49(2), June 2023.

[BG19] Aleksandar Bojchevski and Stephan Günnemann. Certifiable robustness to graph perturbations. In *NeurIPS*, 2019.

[BK24] Houssem Ben Braiek and Foutse Khomh. Machine learning robustness: A primer, 2024.

[BLMT24] Michael Benedikt, Chia-Hsuan Lu, Boris Motik, and Tony Tan. Decidability of graph neural networks via logical characterizations. In *ICALP 2024*, pages 127:1–127:20, 2024.

[DMA⁺15] David Duvenaud, Dougal Maclaurin, Jorge Aguilera-Iparraguirre, Rafael Gómez-Bombarelli, Timothy Hirzel, Alán Aspuru-Guzik, and Ryan P. Adams. Convolutional networks on graphs for learning molecular fingerprints. In *NeurIPS*, 2015.

[FBZA22] Ben Finkelshtein, Chaim Baskin, Evgenii Zheltonozhskii, and Uri Alon. Single-node attacks for fooling graph neural networks. *Neurocomputing*, 513:1–12, 2022.

[FL19] Matthias Fey and Jan E. Lenssen. Fast graph representation learning with PyTorch Geometric. *arXiv:1903.02428*, 2019.

[GSR⁺17] Justin Gilmer, Samuel S. Schoenholz, Patrick F. Riley, Oriol Vinyals, and George E. Dahl. Neural message passing for quantum chemistry. In *ICML*, 2017.

[Gün22] Stephan Günnemann. *Graph Neural Networks: Adversarial Robustness*. Springer Singapore, 2022.

[Gur24] Gurobi Optimization, LLC. Gurobi Optimizer Reference Manual, 2024.

[HYL17] William L. Hamilton, Zhitao Ying, and Jure Leskovec. Inductive representation learning on large graphs. In *NeurIPS*, 2017.

[HZCM24] Christopher Hojny, Shiqiang Zhang, Juan S. Campos, and Ruth Misener. Verifying message-passing neural networks via topology-based bounds tightening. In *ICML*, 2024.

[JSPZ20] Hongwei Jin, Zhan Shi, Venkata Jaya Shankar Ashish Peruri, and Xinhua Zhang. Certified robustness of graph convolution networks for graph classification under topological attacks. In *NeurIPS*, 2020.

[KBD⁺17] Guy Katz, Clark W. Barrett, David L. Dill, Kyle Julian, and Mykel J. Kochenderfer. Reluplex: An efficient SMT solver for verifying deep neural networks. In *CAV*, 2017.

[KHI⁺19] Guy Katz, Derek A. Huang, Duligur Ibeling, Kyle Julian, Christopher Lazarus, Rachel Lim, Parth Shah, Shantanu Thakoor, Haoze Wu, Aleksandar Zeljic, David L. Dill, Mykel J. Kochenderfer, and Clark Barrett. The Marabou Framework for Verification and Analysis of Deep Neural Networks. In *CAV*, 2019.

[KMB⁺16] Steven M. Kearnes, Kevin McCloskey, Marc Berndl, Vijay S. Pande, and Patrick Riley. Molecular graph convolutions: moving beyond fingerprints. *Journal of Computer Aided Molecular Design*, 30(8):595–608, 2016.

[LDX⁺24] Chang Liu, Yinpeng Dong, Wenzhao Xiang, Xiao Yang, Hang Su, Jun Zhu, Yuefeng Chen, Yuan He, Hui Xue, and Shibao Zheng. A comprehensive study on robustness of image classification models: Benchmarking and rethinking. *Int. J. Comput. Vision*, 133(2):567–589, August 2024.

[LEA25] Tobias Ladner, Michael Eichelbeck, and Matthias Althoff. Formal verification of graph convolutional networks with uncertain node features and uncertain graph structure. *Trans. Mach. Learn. Res.*, 2025, 2025.

[LGCR22] Nikolaos Louloudakis, Perry Gibson, Jose Cano, and Ajitha Rajan. Assessing robustness of image recognition models to changes in the computational environment. In *NeurIPS ML Safety Workshop*, 2022.

- [LZPZ24] Yuni Lai, Yulin Zhu, Bailin Pan, and Kai Zhou. Node-aware bi-smoothing: Certified robustness against graph injection attacks. In *IEEE SP*, 2024.
- [MKB⁺20] Christopher Morris, Nils M. Kriege, Franka Bause, Kristian Kersting, Petra Mutzel, and Marion Neumann. TUDataset: A collection of benchmark datasets for learning with graphs. *ArXiv*, abs/2007.08663, 2020.
- [MLK25] Chia-Hsuan Lu Minghao Liu and Marta Kwiatkowska. Exact verification of graph neural networks with incremental constraint solving, 2025. <https://www.arxiv.org/abs/2508.09320>.
- [NSST24] Pierre Nunn, Marco Sälzer, François Schwarzenbuber, and Nicolas Troquard. A logic for reasoning about aggregate-combine graph neural networks. In *IJCAI 2024*, pages 3532–3540, 2024.
- [PWC⁺20] Hongbin Pei, Bingzhen Wei, Kevin Chen-Chuan Chang, Yu Lei, and Bo Yang. Geom-gcn: Geometric graph convolutional networks. In *International Conference on Learning Representations (ICLR)*, 2020.
- [SBV21] Jonathan Shlomi, Peter Battaglia, and Jean-Roch Vlimant. Graph neural networks in particle physics. *Machine Learning: Science and Technology*, 2(2):021001, 2021.
- [SL21] Marco Sälzer and Martin Lange. Reachability is np-complete even for the simplest neural networks. In *RP*, 2021.
- [SL23] Marco Sälzer and Martin Lange. Fundamental limits in formal verification of message-passing neural networks. In *ICLR*, 2023.
- [SNB⁺08] Prithviraj Sen, Galileo Namata, Mustafa Bilgic, Lise Getoor, Brian Gallagher, and Tina Eliassi-Rad. Collective classification in network data. *AI Mag.*, 29(3):93–106, September 2008.
- [YSX⁺23] Renchi Yang, Jieming Shi, Xiaokui Xiao, Yin Yang, Sourav S. Bhowmick, and Juncheng Liu. PANE: scalable and effective attributed network embedding. *The VLDB Journal*, 32(6):1237–1262, March 2023.
- [ZAG18] Daniel Zügner, Amir Akbarnejad, and Stephan Günnemann. Adversarial attacks on neural networks for graph data. In *KDD*, 2018.
- [ZG20] Daniel Zügner and Stephan Günnemann. Certifiable robustness of graph convolutional networks under structure perturbations. In *KDD*, 2020.

A Variant of the high-level algorithm for computing the radius of satisfaction

To compute the radius of satisfaction, we can exhaustively search for the radius under the guidance of the partial oracle. There are four cases.

- If `OracleResult` is `UNSAT`, then no normal graph satisfies the condition. By definition, d_m itself is the radius.
- If `OracleResult` is `SAT` and $d_m = 0$, then there exists a completion \mathcal{G}' of \mathcal{H} with $\text{dist}(\mathcal{G}', \mathcal{G}) = \text{dist}(\mathcal{H}, \mathcal{G})$, which implies that the radius is -1 .
- If `OracleResult` = `SAT` and $d_m > 0$, then the infimum must be strictly less than d_m . In this case the algorithm proceeds recursively with budget $d_m - 1$.
- If `OracleResult` = `UNKNOWN`, then the algorithm converts an unknown edge to either a non-edge or a normal edge and proceeds recursively.

We now formalize this by presenting a variant of the high-level algorithm for computing the radius for satisfaction (Algorithm 2). It exhaustively searches for the smallest $d \leq d_m$ such that the partial oracle returns `UNSAT`. The manner in which the partial oracle is used is the same as in Algorithm 1.

The correctness of Algorithm 2 can be established by induction on the sum $d_m + |E^{\text{Unk}}|$.

- If `OracleResult` is `UNSAT`, then no normal graph satisfies the condition. By definition, d_m itself is the infimum.
- If `OracleResult` is `SAT` and $d_m = 0$, then there exists a completion \mathcal{G}' of \mathcal{H} with $\text{dist}(\mathcal{G}', \mathcal{G}) = \text{dist}(\mathcal{H}, \mathcal{G})$, which implies that there is no such infimum.

For the induction step:

Algorithm 2 Algorithm for computing the radius of satisfaction.

```

1: procedure SEARCH( $\mathcal{Q}, \mathcal{G}, v, \mathcal{H}, d_m$ )
2:   OracleResult  $\leftarrow \mathcal{O}_{\mathcal{Q}, \mathcal{G}, v}(\mathcal{H}, d_m)$ .
3:   if OracleResult is SAT then
4:     if  $d_m$  is 0 then
5:       return -1
6:     else
7:       return SEARCH( $\mathcal{Q}, \mathcal{G}, v, \mathcal{H}, d_m - 1$ )
8:     end if
9:   else if OracleResult is UNSAT then
10:    return  $d_m$ 
11:   else
12:     Pick  $e \in E_{\text{Unk}}$ .
13:     if  $e$  is an edge in  $\mathcal{G}$  then
14:        $\mathcal{H}_1 \leftarrow \mathcal{H}$  by converting  $e$  into a normal edge.
15:        $\mathcal{H}_2 \leftarrow \mathcal{H}$  by converting  $e$  into a non-edge.
16:     else
17:        $\mathcal{H}_1 \leftarrow \mathcal{H}$  by converting  $e$  into a non-edge.
18:        $\mathcal{H}_2 \leftarrow \mathcal{H}$  by converting  $e$  into a normal edge.
19:     end if
20:      $d_1 \leftarrow \text{SEARCH}(\mathcal{Q}, \mathcal{G}, v, \mathcal{H}_1, d_m)$ 
21:      $d_2 \leftarrow \text{SEARCH}(\mathcal{Q}, \mathcal{G}, v, \mathcal{H}_2, d_m - 1)$ 
22:     return  $\min(d_1, d_2 + 1)$ 
23:   end if
24: end procedure

```

- If OracleResult = SAT and $d_m > 0$, then the infimum must be strictly less than d_m . By the induction hypothesis, it coincides with the result for $d_m - 1$.
- If OracleResult = UNKNOWN, then the maximum budget is the minimum of the budgets obtained from \mathcal{H}_1 with parameter d_m and from \mathcal{H}_2 with parameter $d_m - 1$. Our choice of \mathcal{H}_1 and \mathcal{H}_2 ensures that for every completion \mathcal{G}_1 of \mathcal{H}_1 , $\text{dist}(\mathcal{G}_1, \mathcal{H}_1) = \text{dist}(\mathcal{G}', \mathcal{H})$, and for every completion \mathcal{G}_2 of \mathcal{H}_2 , $\text{dist}(\mathcal{G}_2, \mathcal{H}_2) = \text{dist}(\mathcal{G}', \mathcal{H}) + 1$. Moreover, we have $\text{COMP}(\mathcal{H}) = \text{COMP}(\mathcal{H}_1) \cup \text{COMP}(\mathcal{H}_2)$.

B Variants of algorithms for graph classification

Recall that in the paper body, we focused on GNNs as node classifiers. However, we mentioned that GNNs can also be used as graph classifiers, by applying additional pooling and linear transformation layers within a final layer. We now explain this in detail, focusing on sum pooling, where the final outcome depends on the summation of the last-layer features of each vertex. Here, we provide the formal definitions and the adversarial robustness problem for this type of task.

Definition 18 (Graph classifier induced by a GNN). Let \mathcal{A} be an L -layer GNN and $\mathcal{G} \in \mathfrak{G}_{V,X}$. For the entire graph \mathcal{G} , the predicted class of \mathcal{A} , denoted by $\hat{c}(\mathcal{G})$, is

$$\hat{c}(\mathcal{G}) := \arg \max_{1 \leq i \leq d^{(L+1)}} \left(\mathbf{C}^{(L+1)} \sum_{v \in V} \xi_{\mathcal{G}}^{(L)}(v) + \mathbf{b}^{(L+1)} \right) [i],$$

where $\mathbf{C}^{(L+1)} \in \mathbb{R}^{d^{(L+1)} \times d^{(L)}}$ and $\mathbf{b}^{(L+1)} \in \mathbb{R}^{d^{(L+1)}}$ are extra learnable coefficient matrix and bias vector.

Definition 19 (Adversarial robustness radius of graph classify GNNs). Let \mathcal{A} be an L -layer GNN, \mathcal{G} a graph, $F \subseteq V \times V$ a set of edges, $\Delta \in \mathbb{N}$ a global budget, and $\delta \in \mathbb{N}$ a local budget. For a class $1 \leq c \leq d^{(L)}$, we define the adversarial robustness radius of \mathcal{A} with respect to c as follows:

For the entire graph \mathcal{G} , we say that \mathcal{A} is adversarially robust for \mathcal{G} with class c if, for every perturbed normal graph $\mathcal{G}' \in \mathfrak{Q}(\mathcal{G}, F, \Delta, \delta)$, it holds that $\hat{c}(\mathcal{G}') = c$.

Note that the condition in the above definition is equivalent to requiring that, for every $1 \leq c' \neq c \leq d^{(L)}$,

$$\left(\mathbf{C}^{(L+1)} \sum_{v \in V} \xi_{\mathcal{G}'}^{(L)}(v) + \mathbf{b}^{(L+1)} \right) [c] \geq \left(\mathbf{C}^{(L+1)} \sum_{v \in V} \xi_{\mathcal{G}'}^{(L)}(v) + \mathbf{b}^{(L+1)} \right) [c'].$$

As with node classification, we also consider a weaker notion of adversarial robustness, in which the target class c' is fixed in advance.

Regarding the partial oracle for graph classification, the non-robustness tester is straightforward. For the bound propagator, we can extend the bound propagation rules to apply to the pooling and linear layers. Specifically, we define

$$\begin{aligned}\bar{\xi}_{\mathcal{H}}^{(L+1)} &= \text{relax} \left(\mathbf{C}^{(L+1)}, \sum_{v \in V} \bar{\xi}_{\mathcal{H}}^{(L)}(v), \sum_{v \in V} \underline{\xi}_{\mathcal{H}}^{(L)}(v) \right) + \mathbf{b}^{(L+1)} \\ \underline{\xi}_{\mathcal{H}}^{(L+1)} &= \text{relax} \left(\mathbf{C}^{(L+1)}, \sum_{v \in V} \bar{\xi}_{\mathcal{H}}^{(L)}(v), \sum_{v \in V} \underline{\xi}_{\mathcal{H}}^{(L)}(v) \right) + \mathbf{b}^{(L+1)}.\end{aligned}$$

By applying Lemma 2, we can establish the desired correctness condition: for every $\mathcal{G}' \subseteq \mathcal{H}$,

$$\underline{\xi}_{\mathcal{H}}^{(L+1)} \leq \mathbf{C}^{(L+1)} \sum_{v \in V} \xi_{\mathcal{G}'}^{(L)}(v) + \mathbf{b}^{(L+1)} \leq \bar{\xi}_{\mathcal{H}}^{(L+1)}.$$

C Variation of the algorithms for undirected graphs

Recall that in the body of the paper, we presented our results for a data model consisting of directed graphs, where the GNNs aggregated over incoming neighbors only. We mentioned that this model is commonly used in prior papers on GNN robustness, but that it is more common in the graph learning literature as a whole to work with undirected graphs, and with a GNN variant that aggregates over (undirected) neighbors.

We explain that very little needs to change for the undirected variant. In general, the algorithm and oracle described in Section 3 remain the same for both directed and undirected graphs. The main adjustment lies in how features and bounds are propagated when the optimization strategy for incremental computation is applied. For a directed graph, if we convert an edge from u to v , we only need to update the features and bounds of vertex v at the first layer; in the second layer, the update is propagated to the neighbors of v . However, for an undirected GNN, we need to update both u and v at the first layer, and then propagate the updates to the neighbors of both u and v in subsequent layers.

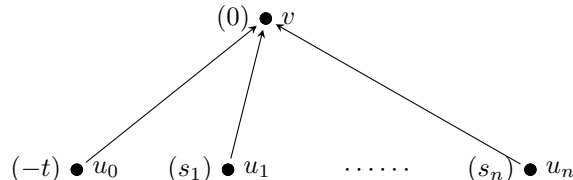
D Missing proofs

D.1 Proof of coNP-completeness of robustness problem

In this section, we will prove that checking the adversarial robustness of GNNs is coNP-complete. For aggregation function **sum** and **mean** we show that there is a GNN \mathcal{A} using **sum** (**mean**, resp.) such that the problem of checking whether \mathcal{A} is adversarially robust for a given node in a graph is coNP-complete. For aggregation function **max**, the GNN \mathcal{A} is part of the input.

Note that membership in coNP is straightforward for every GNN \mathcal{A} , so we will focus on the hardness. All reductions are from the subset-sum problem: Given a set of positive integers $S = \{s_1, s_2, \dots, s_n\}$ and a positive integer t , decide whether there exists a subset $S_0 \subseteq S$ such that the sum of the integers in S_0 is exactly t . This problem is known to be NP-complete.

For aggregation function sum Given an instance of subset-sum problem $S = \{s_1, \dots, s_n\}$ and t as above, consider the following graph \mathcal{G} :



On each node, the left side is the feature value and the right side is the node name. The initial feature of each vertex is 1-dimensional, where $X(u_i) = s_i$ for $1 \leq i \leq n$, $X(u_0) = -t$ and $X(v) = 0$. All edges are fragile edges and the global budget $\Delta = n$.

The GNN \mathcal{A} has two layers, where $d^{(0)} = 1$, $d^{(1)} = 2$ and $d^{(2)} = 2$. On perturbed graph $\mathcal{G}' \in \mathfrak{Q}(\mathcal{G}, F, \Delta)$, we describe the computation of \mathcal{A} on $\langle \mathcal{G}', v \rangle$ layer by layer. In the first layer, the GNN \mathcal{A} computes $\xi_{\mathcal{G}'}^{(1)}(v)$:

$$\xi_{\mathcal{G}'}^{(1)}(v) = \text{ReLU} \left(\frac{\sum_{u \in \mathcal{N}_{\mathcal{G}'}(v)} X(u)}{\sum_{u \in \mathcal{N}_{\mathcal{G}'}(v)} -X(u)} \right)$$

In the second layer, the GNN \mathcal{A} computes $\xi_{\mathcal{G}'}^{(2)}(v)$:

$$\xi_{\mathcal{G}'}^{(2)}(v) = \text{ReLU} \left(\frac{1/2}{\xi_{\mathcal{G}'}^{(1)}(v)[1] + \xi_{\mathcal{G}'}^{(1)}(v)[2]} \right)$$

Note that $\xi_{\mathcal{G}'}^{(2)}(v)[1]$ is always $1/2$. Since all s_1, \dots, s_n and t are positive integers, we have $\xi_{\mathcal{G}'}^{(2)}(v)[2] > 1/2$. Thus, $\hat{c}(\mathcal{G}, v) = 2$.

We claim that \mathcal{A} is not adversarially robust for v with class 1 iff the subset-sum instance S and t has a solution. To see this, suppose that the subset-sum instance S and t has a solution. Suppose that $S_0 \subseteq S$ is such a solution, i.e. $\sum_{s \in S_0} s = t$. Consider $\mathcal{G}' \in \mathfrak{Q}(\mathcal{G}, F, \Delta)$ where the set of edges $E' = \{(u_0, v)\} \cup \{(u_i, v) \mid s_i \in S_0\}$. Then, we have $\xi_{\mathcal{G}'}^{(2)}(v) = (1/2, 0)$. Thus, $\hat{c}(\mathcal{G}', v) = 1$.

For the converse, we will use the identity that $\text{ReLU}(a) + \text{ReLU}(-a) = |a|$, for every real number $a \in \mathbb{R}$. Suppose that \mathcal{A} is not adversarially robust for v with class 1. Then, there is a perturbed graph $\mathcal{G}' \in \mathfrak{Q}(\mathcal{G}, F, \Delta)$, such that $\hat{c}(\mathcal{G}', v) = 1$. By definition, $\xi_{\mathcal{G}'}^{(2)}(v)[1] > \xi_{\mathcal{G}'}^{(2)}(v)[2]$. Since all s_1, \dots, s_n and t are positive integers and $\xi_{\mathcal{G}'}^{(2)}(v)[1] = 1/2$, we have $\xi_{\mathcal{G}'}^{(2)}(v)[2] = 0$. Since by the definition,

$$\xi_{\mathcal{G}'}^{(2)}(v)[2] = \text{ReLU} \left(\sum_{u \in \mathcal{N}_{\mathcal{G}'}(v)} X(u) \right) + \text{ReLU} \left(\sum_{u \in \mathcal{N}_{\mathcal{G}'}(v)} -X(u) \right) = \left| \sum_{u \in \mathcal{N}_{\mathcal{G}'}(v)} X(u) \right|$$

we have:

$$\sum_{u \in \mathcal{N}_{\mathcal{G}'}(v)} X(u) = 0$$

This implies that there is $S_0 \subseteq S$ such that $t = \sum_{s \in S_0} s$.

For aggregation function mean The reduction is exactly the same as the case for **sum**. Given a set of positive integers $S = \{s_1, \dots, s_n\}$ and a positive integer t , we construct the graph \mathcal{G} , the set of fragile edges F and the global budget Δ in a similar manner as in the previous case. The difference is in the initial feature of each vertex, where $X(u_i) = (n+1)s_i$ for $1 \leq i \leq n$, $X(u_0) = -(n+1)t$ and $X(v) = 0$.

The GNN \mathcal{A} uses aggregation function **mean**. On perturbed graph $\mathcal{G}' \in \mathfrak{Q}(\mathcal{G}, F, \Delta)$, it computes $\xi_{\mathcal{G}'}^{(1)}(v)$ in the first layer:

$$\xi_{\mathcal{G}'}^{(1)}(v) = \text{ReLU} \left(\frac{\text{mean}(\{X(u) \mid u \in \mathcal{N}_{\mathcal{G}'}(v)\})}{\text{mean}(\{-X(u) \mid u \in \mathcal{N}_{\mathcal{G}'}(v)\})} \right)$$

The second layer is exactly the same as in the case of **sum**. We observe that for every subset $S_0 \subseteq S$:

– If $t = \sum_{s \in S_0} s$, then

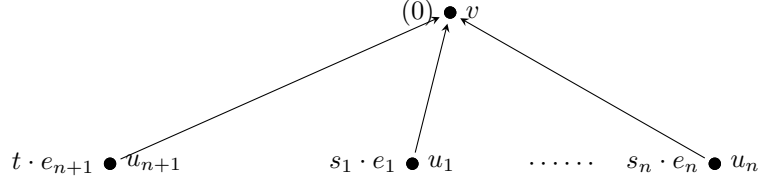
$$\frac{(n+1)t}{|S_0|} - \frac{\sum_{s \in S_0} (n+1)s}{|S_0| + 1} = \frac{n+1}{|S_0| + 1} \left(t - \sum_{s \in S_0} s \right) = 0$$

– If $t \neq \sum_{s \in S_0} s$, then

$$\left| \frac{(n+1)t}{|S_0| + 1} - \frac{\sum_{s \in S_0} (n+1)s}{|S_0| + 1} \right| = \frac{n+1}{|S_0| + 1} \left| t - \sum_{s \in S_0} s \right| \geq 1.$$

To establish correctness of the reduction, we note that the term $\frac{n+1}{|S_0| + 1} |t - \sum_{s \in S_0} s|$ is precisely $\xi_{\mathcal{G}'}^{(2)}(v)[2]$, where $\mathcal{G}' \in \mathfrak{Q}(\mathcal{G}, F, \Delta)$ is the perturbed graph.

For aggregation function **max** The reduction is also similar to the case for **sum**, except that the GNN \mathcal{A} is no longer fixed. Given an instance of subset-sum problem $S = \{s_1, \dots, s_n\}$ and t as above, we construct the following graph \mathcal{G} :



where $e_i \in \mathbb{R}^{n+1}$ is the unit vector in \mathbb{R}^{n+1} with 1 in the i -th coordinate and 0 elsewhere. The set of fragile edges is $F = \{(v, u_1), (v, u_2), \dots, (v, u_n)\}$. The global budget $\Delta = n$.

We construct the GNN \mathcal{A} with three layers, where $d^{(0)} = n+1$, $d^{(1)} = n+1$, $d^{(2)} = 2$ and $d^{(3)} = 2$. Note that the dimension $d^{(0)} = d^{(1)} = n+1$, which depends on the subset-sum instance. On perturbed graph $\mathcal{G}' \in \mathfrak{Q}(\mathcal{G}, F, \Delta)$, we describe the computation of \mathcal{A} on $\langle \mathcal{G}', v \rangle$ layer by layer. In the first layer, the GNN \mathcal{A} computes $\xi_{\mathcal{G}'}^{(1)}(v)$:

$$\xi_{\mathcal{G}'}^{(1)}(v) = \text{ReLU} \left(\max \left\{ \xi_{\mathcal{G}'}^{(0)}(u) \mid u \in \mathcal{N}_{\mathcal{G}'}(v) \right\} \right)$$

In the second layer, the GNN \mathcal{A} computes $\xi_{\mathcal{G}'}^{(2)}(v)$:

$$\xi_{\mathcal{G}'}^{(2)}(v) = \text{ReLU} \left(\frac{\xi_{\mathcal{G}'}^{(1)}(v)[n+1] - \sum_{i=1}^n \xi_{\mathcal{G}'}^{(1)}(v)[i]}{\sum_{i=1}^n \xi_{\mathcal{G}'}^{(1)}(v)[i] - \xi_{\mathcal{G}'}^{(1)}(v)[n+1]} \right)$$

In the third layer, the GNN \mathcal{A} computes $\xi_{\mathcal{G}'}^{(3)}(v)$:

$$\xi_{\mathcal{G}'}^{(3)}(v) = \text{ReLU} \left(\frac{1/2}{\xi_{\mathcal{G}'}^{(2)}(v)[1] + \xi_{\mathcal{G}'}^{(2)}(v)[2]} \right)$$

Note that in the second and third layer in this GNN are similar to the first and second layer in the GNN for **sum**. The first layer in this case the GNN simply computes the vector (b_1, \dots, b_{n+1}) that corresponds to a subset $S_0 \subseteq S$ where $b_i = s_i$ if $s_i \in S_0$ and $b_i = 0$ otherwise, and $b_{n+1} = t$.

In a manner similar to the **sum** case, we can show that that \mathcal{A} is not adversarially robust for v with class 1 iff the subset-sum instance S and t has a solution.

D.2 Proof of Lemma 1

Recall Lemma 1:

For every incomplete graph $\mathcal{H} \in \mathfrak{H}_{V,X}$ and graph $\mathcal{G} \in \mathfrak{H}_{V,X}$, letting \mathcal{G}' be the grounding of \mathcal{H} to \mathcal{G} , $\text{dist}(\mathcal{G}', \mathcal{G}) = \text{dist}(\mathcal{H}, \mathcal{G})$.

Proof. For every $(v, u) \in V \times V$, if (v, u) is inconsistent between \mathcal{H} and \mathcal{G} , then either (v, u) is an edge in \mathcal{H} and a non-edge in \mathcal{G} , or (v, u) is a non-edge in \mathcal{H} and an edge in \mathcal{G} . Note that by the definition of the grounding, if (v, u) is an edge in \mathcal{H} , then is also an edge in \mathcal{G}' ; if (v, u) is a non-edge in \mathcal{H} , then is also a non-edge in \mathcal{G}' . Thus, for both cases, (v, u) is inconsistent between \mathcal{G}' and \mathcal{G} .

On the other hand, if (v, u) is consistent between \mathcal{H} and \mathcal{G} , then either (v, u) is a unknown edge in \mathcal{H} , or (v, u) is the same type of edge in both \mathcal{H} and \mathcal{G} . For both cases, by the definition of grounding, (v, u) are consistent between \mathcal{G}' and \mathcal{G} . Thus, $\text{dist}(\mathcal{G}', \mathcal{G}) = \text{dist}(\mathcal{H}, \mathcal{G})$.

D.3 Proof of Lemma 2

Recall Lemma 2:

For every graph $\mathcal{G} \in \mathfrak{H}_{V,X}$ and every set E_p of pairs of nodes, \mathcal{G} is a completion of its relaxation with respect to E_p , and hence $\text{dist}(\mathcal{H}_{\mathcal{G}, E_p}, \mathcal{G}) = 0$.

Proof. For every $(v, u) \in V \times V$, by the definition of relaxation, one of the following three cases hold.

- (v, u) is an edge in \mathcal{G} and an edge $\mathcal{H}_{\mathcal{G}, E_p}$.
- (v, u) is a non-edge in \mathcal{G} and a non-edge $\mathcal{H}_{\mathcal{G}, E_p}$.
- $(v, u) \in E_p$ and it is a unknown edge $\mathcal{H}_{\mathcal{G}, E_p}$.

For all cases, (v, u) is consistent between $\mathcal{H}_{\mathcal{G}, E_p}$ and \mathcal{G} . Therefore, \mathcal{G} is a completion, and the distance between them is zero.

D.4 Proof of the correctness of Algorithm 1

Recall the high-level algorithm, Algorithm 1, for solving the d radius satisfaction problem using a partial oracle. We will show that the algorithm is correct by induction on $|E^{\text{Unk}}|$.

The base case is $|E^{\text{Unk}}| = 0$. In this case, by definition, the oracle always outputs SAT or UNSAT and the correctness follows immediately.

For the induction step, we note that the number of unknown edges in \mathcal{H}_1 and \mathcal{H}_2 decreases by 1. Thus, the correctness follows immediately from the induction hypothesis.

D.5 Proof of Lemma 3

Recall Lemma 3:

For every $\mathbf{A} \in \mathbb{R}^{m \times n}$ and $\bar{\mathbf{v}}, \mathbf{v}, \underline{\mathbf{v}} \in \mathbb{R}^n$ with $\underline{\mathbf{v}} \leq \mathbf{v} \leq \bar{\mathbf{v}}$, it holds that

$$\underline{\text{relax}}(\mathbf{A}, \bar{\mathbf{v}}, \underline{\mathbf{v}}) \leq \mathbf{A} \cdot \mathbf{v} \leq \bar{\text{relax}}(\mathbf{A}, \bar{\mathbf{v}}, \underline{\mathbf{v}}).$$

Proof. For $1 \leq i \leq m$, note that

$$\begin{aligned} (\mathbf{A} \cdot \mathbf{v})_i &= \sum_{1 \leq j \leq n} (\max(\mathbf{A}_{i,j}, 0) + \min(\mathbf{A}_{i,j}, 0)) \mathbf{v}_j \\ &\leq \sum_{1 \leq j \leq n} (\max(\mathbf{A}_{i,j}, 0) \bar{\mathbf{v}}_j) + (\min(\mathbf{A}_{i,j}, 0) \underline{\mathbf{v}}_j) \\ &= (\mathbf{A}^+ \cdot \bar{\mathbf{v}})_i + (\mathbf{A}^- \cdot \underline{\mathbf{v}})_i \end{aligned}$$

The lower bound can be proved analogously.

D.6 Proof of Lemma 4

Recall Lemma 4:

For every completion \mathcal{G}' of \mathcal{H} , $0 \leq \ell \leq L$, and vertex $v \in V$, it holds that

$$\underline{\xi}_{\mathcal{H}}^{(\ell)}(v) \leq \xi_{\mathcal{G}'}^{(\ell)}(v) \leq \bar{\xi}_{\mathcal{H}}^{(\ell)}(v) \quad (1)$$

Proof. The proof is by induction on layers. For the base case $\ell = 0$, notice that for every completion \mathcal{G}' of \mathcal{H} , $\xi_{\mathcal{G}'}^{(0)}(v) = X(v)$. Thus, it is clear that (1) holds.

For the induction step $1 \leq \ell \leq L$, it suffices to prove the relaxation for the aggregation functions:

$$\underline{\text{aggr}}\left(\underline{S}^{\text{Norm}}, \underline{S}^{\text{Unk}}\right) \leq \text{aggr}\left(\left\{\xi_{\mathcal{G}}^{(\ell-1)}(u) \mid u \in \mathcal{N}_{\mathcal{G}}(v)\right\}\right) \leq \bar{\text{aggr}}\left(\bar{S}^{\text{Norm}}, \bar{S}^{\text{Unk}}\right). \quad (2)$$

The remainder then follows from Lemma 3.

Since \mathcal{G}' is a completion of \mathcal{H} , we have

$$\mathcal{N}_{\mathcal{H}}^{\text{Norm}}(v) \subseteq \mathcal{N}_{\mathcal{G}'}(v) \subseteq \mathcal{N}_{\mathcal{H}}^{\text{Norm}}(v) \cup \mathcal{N}_{\mathcal{H}}^{\text{Unk}}(v).$$

The proof for the lower bound is symmetric; here we focus only on the upper bound.

- Suppose that **aggr** is **sum**. Then

$$\begin{aligned}
\mathbf{sum} \left(\left\{ \xi_{\mathcal{G}}^{(\ell-1)}(u) \mid u \in \mathcal{N}_{\mathcal{G}}(v) \right\} \right) &= \sum_{u \in \mathcal{N}_{\mathcal{G}'}(v)} \xi_{\mathcal{G}'}^{(\ell-1)}(u) \\
&\leq \sum_{u \in \mathcal{N}_{\mathcal{H}}^{\text{Norm}}(v)} \bar{\xi}_{\mathcal{H}}^{(\ell-1)}(u) + \sum_{u \in \mathcal{N}_{\mathcal{G}'}(v) \cap \mathcal{N}_{\mathcal{H}}^{\text{Unk}}(v)} \bar{\xi}_{\mathcal{H}}^{(\ell-1)}(u) \\
&\leq \sum_{u \in \mathcal{N}_{\mathcal{H}}^{\text{Norm}}(v)} \bar{\xi}_{\mathcal{H}}^{(\ell-1)}(u) + \sum_{u \in \mathcal{N}_{\mathcal{H}}^{\text{Unk}}(v)} \max \left(\bar{\xi}_{\mathcal{H}}^{(\ell-1)}(u), 0 \right) \\
&= \overline{\mathbf{sum}} \left(\bar{S}^{\text{Norm}}, \bar{S}^{\text{Unk}} \right).
\end{aligned}$$

Note that by the induction hypothesis, $\xi_{\mathcal{G}'}^{(\ell-1)}(u) \leq \bar{\xi}_{\mathcal{H}}^{(\ell-1)}(u)$.

- Suppose that **aggr** is **max**. Inequality (2) can be established by a straightforward case analysis.
- Suppose that **aggr** is **mean**. Let k be the cardinality of the set $\mathcal{N}_{\mathcal{G}'}(v) \cap \mathcal{N}_{\mathcal{H}}^{\text{Unk}}(v)$, and let s_1, \dots, s_k be the k -largest element in \bar{S}^{Unk} .

$$\begin{aligned}
\sum_{u \in \mathcal{N}_{\mathcal{G}'}(v)} \xi_{\mathcal{G}'}^{(\ell-1)}(u) &\leq \sum_{u \in \mathcal{N}_{\mathcal{H}}^{\text{Norm}}(v)} \bar{\xi}_{\mathcal{H}}^{(\ell-1)}(u) + \sum_{u \in \mathcal{N}_{\mathcal{G}'}(v) \cap \mathcal{N}_{\mathcal{H}}^{\text{Unk}}(v)} \bar{\xi}_{\mathcal{H}}^{(\ell-1)}(u) \\
&\leq \sum_{u \in \mathcal{N}_{\mathcal{H}}^{\text{Norm}}(v)} \bar{\xi}_{\mathcal{H}}^{(\ell-1)}(u) + \sum_{1 \leq j \leq k} s_j
\end{aligned}$$

Consequently,

$$\begin{aligned}
\mathbf{mean} \left(\left\{ \xi_{\mathcal{G}}^{(\ell-1)}(u) \mid u \in \mathcal{N}_{\mathcal{G}}(v) \right\} \right) &\leq \left(\sum_{u \in \mathcal{N}_{\mathcal{H}}^{\text{Norm}}(v)} \bar{\xi}_{\mathcal{H}}^{(\ell-1)}(u) + \sum_{1 \leq j \leq k} s_j \right) / (|\mathcal{N}_{\mathcal{H}}^{\text{Norm}}(v)| + k) \\
&\leq \overline{\mathbf{mean}} \left(\bar{S}^{\text{Norm}}, \bar{S}^{\text{Unk}} \right).
\end{aligned}$$

E Budge-specific experimental results

Recall that tables 2 and 6 in the main text reports results summed over different budgets. Here, we provide additional details on the experimental results for each individual budget.

E.1 End to end performance on node classification

Table 7 to Table 10 present detailed comparison results of ROBLIGHT, GNNEV, and SCIP-MPNN for both weak and general robustness on the Cora, CiteSeer, Cornell, Texas, and Wisconsin datasets, using various aggregation functions and perturbation budgets. All experiments are conducted on node classification tasks, where the fragile set of edges is restricted to deletions only, and the local budget is set equal to the global budget. Note that SCIP-MPNN only supports weak robustness for the **sum** aggregation. t_a denotes the average runtime, and t_g denotes the shifted geometric mean of the runtime.

E.2 End to end performance on graph classification

Table 11 to Table 16 present detailed comparison results of ROBLIGHT and SCIP-MPNN for both weak and general robustness on the MUTAG and ENZYME datasets, using various aggregation functions and perturbation budgets. All experiments are conducted on graph classification tasks, where the fragile set includes all pairs of vertices excluding self-loops. Note that SCIP-MPNN only supports weak robustness for the **sum** aggregation. t_a denotes the average runtime, and t_g denotes the shifted geometric mean of the runtime.

Table 7: Detailed comparison results of ROBLIGHT, GNNEV, and SCIP-MPNN for weak and general robustness on the Cora, CiteSeer, Cornell, Texas, and Wisconsin datasets with various aggregation functions with global and local budgets $\Delta = 1$. Note that SCIP-MPNN only implements weak robustness for **sum** aggregation. t_a denotes the average runtime, and t_g denotes the shifted geometric mean of the runtime.

		ROBLIGHT						GNNEV						SCIP-MPNN						
		All instances		Robust instances		All instances		Robust instances		All instances		Robust instances		All instances		Robust instances		All instances		
#Instances		#Solved	$t_a(s)$	$t_g(s)$	#Solved	$t_a(s)$	$t_g(s)$	#Solved	$t_a(s)$	$t_g(s)$	#Solved	$t_a(s)$	$t_g(s)$	#Solved	$t_a(s)$	$t_g(s)$	#Solved	$t_a(s)$	$t_g(s)$	
sum (Weak)	Cora	2708	2,708	0.01	0.01	2,514	0.01	0.01	2,228	21.39	11.19	2,034	22.36	11.33	2,699	27.19	13.12	2,541	25.98	12.58
	CiteSeer	3312	3,312	0.01	0.01	3,116	0.01	0.01	3,121	13.32	7.40	2,916	13.25	7.10	3,305	3.16	1.67	3,126	3.09	1.62
	Cornell	183	183	0.01	0.01	137	0.01	0.01	163	14.72	8.48	117	17.83	9.51	183	14.14	5.66	143	14.70	5.80
	Texas	183	183	0.01	0.01	164	0.01	0.01	173	13.89	7.23	153	13.74	6.67	178	18.12	6.41	162	17.35	5.60
	Wisconsin	251	251	0.01	0.01	230	0.01	0.01	223	18.87	10.33	201	19.10	9.97	243	28.36	9.84	228	28.58	9.76
sum	Cora	2708	2,708	0.01	0.01	2,126	0.01	0.01	2,289	20.23	11.23	1,714	21.34	10.79						
	CiteSeer	3312	3,312	0.01	0.01	2,819	0.01	0.01	3,173	14.45	8.17	2,652	14.71	7.62						
	Cornell	183	183	0.01	0.01	112	0.01	0.01	178	17.81	9.60	105	22.62	10.40						
	Texas	183	183	0.01	0.01	115	0.01	0.01	178	11.36	7.04	101	13.45	7.34						
	Wisconsin	251	251	0.01	0.01	198	0.01	0.01	242	18.82	11.17	181	18.39	9.88						
max	Cora	2708	2,708	0.01	0.01	2,179	0.01	0.01	2,177	123.36	42.39	1,685	117.38	36.42						
	CiteSeer	3312	3,312	0.01	0.01	2,804	0.01	0.01	3,042	100.75	23.76	2,518	92.96	19.80						
	Cornell	183	183	0.01	0.01	114	0.01	0.01	153	42.42	19.49	85	39.47	14.83						
	Texas	183	183	0.01	0.01	156	0.01	0.01	166	87.22	18.58	138	74.72	13.44						
	Wisconsin	251	251	0.01	0.01	205	0.01	0.01	200	135.63	29.91	156	132.31	23.21						
mean	Cora	2708	2,708	0.01	0.01	2,173	0.01	0.01	2,147	22.13	12.97	1,622	23.21	12.66						
	CiteSeer	3312	3,312	0.01	0.01	2,776	0.01	0.01	3,095	13.50	7.88	2,528	13.51	7.18						
	Cornell	183	183	0.01	0.01	132	0.01	0.01	159	17.99	10.30	106	20.72	10.66						
	Texas	183	183	0.01	0.01	129	0.01	0.01	174	15.29	8.46	118	15.41	7.95						
	Wisconsin	251	251	0.01	0.01	188	0.01	0.01	217	25.26	12.62	153	23.35	11.19						

Table 8: Detailed comparison results of ROBLIGHT, GNNEV, and SCIP-MPNN for weak and general robustness on the Cora, CiteSeer, Cornell, Texas, and Wisconsin datasets with various aggregation functions with global and local budgets $\Delta = 2$. Note that SCIP-MPNN only implements weak robustness for **sum** aggregation. t_a denotes the average runtime, and t_g denotes the shifted geometric mean of the runtime.

		ROBLIGHT						GNNEV						SCIP-MPNN						
		All instances		Robust instances		All instances		Robust instances		All instances		Robust instances		All instances		Robust instances		All instances		
#Instances		#Solved	$t_a(s)$	$t_g(s)$	#Solved	$t_a(s)$	$t_g(s)$	#Solved	$t_a(s)$	$t_g(s)$	#Solved	$t_a(s)$	$t_g(s)$	#Solved	$t_a(s)$	$t_g(s)$	#Solved	$t_a(s)$	$t_g(s)$	
sum (Weak)	Cora	2708	2,708	0.01	0.01	2,334	0.01	0.01	1,946	43.89	16.61	1,602	46.57	16.11	2,560	75.19	31.23	2,197	75.28	29.51
	CiteSeer	3312	3,312	0.01	0.01	3,024	0.01	0.01	3,100	18.01	8.47	2,803	17.80	7.81	3,273	13.31	4.41	2,984	12.56	4.00
	Cornell	183	183	0.01	0.01	108	0.01	0.01	155	21.54	10.04	80	22.39	8.30	176	38.92	11.74	103	38.22	10.12
	Texas	183	183	0.01	0.01	152	0.01	0.01	150	19.75	7.25	117	8.41	3.22	170	30.10	9.78	138	22.83	6.24
	Wisconsin	251	251	0.01	0.01	218	0.01	0.01	190	23.38	10.25	154	20.37	8.10	213	50.25	17.05	181	45.03	14.61
sum	Cora	2708	2,708	0.01	0.01	1,777	0.01	0.01	1,920	29.23	12.45	1,101	22.79	7.57						
	CiteSeer	3312	3,312	0.01	0.01	2,620	0.01	0.01	3,097	15.88	8.40	2,372	15.06	6.87						
	Cornell	183	183	0.01	0.01	82	0.01	0.01	161	16.05	8.89	65	14.82	5.97						
	Texas	183	183	0.01	0.01	90	0.01	0.01	156	12.33	6.36	58	2.16	1.42						
	Wisconsin	251	251	0.01	0.01	179	0.01	0.01	200	25.36	10.57	128	17.53	6.30						
max	Cora	2708	2,708	0.01	0.01	1,849	0.01	0.01	1,564	76.71	23.31	955	27.85	7.83						
	CiteSeer	3312	3,312	0.01	0.01	2,652	0.01	0.01	2,705	61.50	19.31	2,078	34.02	12.06						
	Cornell	183	183	0.01	0.01	102	0.01	0.01	133	43.23	18.05	64	30.42	9.95						
	Texas	183	183	0.01	0.01	145	0.01	0.01	134	46.85	10.92	102	3.99	2.66						
	Wisconsin	251	251	0.01	0.01	195	0.02	0.02	139	45.33	12.88	106	20.25	6.52						
mean	Cora	2708	2,708	0.01	0.01	1,816	0.01	0.01	1,689	27.39	11.70	934	22.46	6.66						
	CiteSeer	3312	3,312	0.01	0.01	2,631	0.01	0.01	2,888	16.39	8.05	2,195	15.13	6.37						
	Cornell	183	183	0.01	0.01	116	0.01	0.01	131	10.90	6.76	71	9.62	4.55						
	Texas	183	183	0.01	0.01	114	0.01	0.01	149	17.00	7.21	78	11.72	3.91						
	Wisconsin	251	251	0.01	0.01	172	0.01	0.01	172	22.54	9.47	100	18.32	4.98						

Table 9: Detailed comparison results of ROBLIGHT, GNNEV, and SCIP-MPNN for weak and general robustness on the Cora, CiteSeer, Cornell, Texas, and Wisconsin datasets with various aggregation functions with global and local budgets $\Delta = 5$. Note that SCIP-MPNN only implements weak robustness for **sum** aggregation. t_a denotes the average runtime, and t_g denotes the shifted geometric mean of the runtime.

		ROBLIGHT				GNNEV				SCIP-MPNN			
		All instances		Robust instances		All instances		Robust instances		All instances		Robust instances	
		#Instances	#Solved	$t_a(s)$	$t_g(s)$	#Instances	#Solved	$t_a(s)$	$t_g(s)$	#Instances	#Solved	$t_a(s)$	$t_g(s)$
sum (Weak)	Cora	2708	2,708	0.07	0.06	2,160	0.09	0.08		1,656	23.19	9.71	1,251 21.62 7.76
	CiteSeer	3312	3,311	0.35	0.10	2,938	0.40	0.12		2,990	14.22	7.36	2,620 12.62 6.17
	Cornell	183	183	0.01	0.01	87	0.01	0.01		151	14.22	7.68	67 11.78 5.25
	Texas	183	183	0.55	0.17	144	0.70	0.22		146	11.81	5.37	112 6.33 2.64
	Wisconsin	251	251	2.14	0.69	202	2.66	0.86		175	15.06	7.34	136 10.56 4.92
sum	Cora	2708	2,708	0.03	0.03	1,470	0.06	0.05		1,913	22.52	10.56	962 12.26 4.33
	CiteSeer	3312	3,310	0.31	0.10	2,482	0.41	0.13		3,034	13.36	7.55	2,201 9.43 5.02
	Cornell	183	183	0.01	0.01	72	0.01	0.01		165	12.31	7.93	61 8.99 4.55
	Texas	183	183	0.04	0.03	78	0.10	0.07		159	8.39	5.34	57 1.26 1.09
	Wisconsin	251	251	2.17	0.58	162	3.31	0.88		205	24.15	10.71	119 12.11 4.81
max	Cora	2708	2,707	0.68	0.39	1,548	1.16	0.66		1,645	79.28	24.68	878 12.34 4.68
	CiteSeer	3312	3,299	0.91	0.26	2,512	1.17	0.33		2,621	54.70	16.38	1,958 21.08 8.77
	Cornell	183	183	0.12	0.08	93	0.24	0.16		133	38.32	16.57	59 18.16 7.04
	Texas	183	183	0.96	0.39	139	1.22	0.47		124	22.40	7.32	99 5.73 2.61
	Wisconsin	251	243	2.90	0.87	176	3.12	0.99		140	47.65	12.06	104 8.66 4.77
mean	Cora	2708	2,708	0.01	0.01	1,460	0.02	0.02		1,789	24.25	11.89	842 7.95 3.37
	CiteSeer	3312	3,312	0.22	0.07	2,503	0.28	0.10		2,845	12.58	7.14	2,082 9.35 4.85
	Cornell	183	183	0.01	0.01	101	0.02	0.02		143	13.47	7.95	67 6.47 3.78
	Texas	183	183	0.37	0.13	107	0.63	0.22		149	14.14	6.35	74 9.14 2.77
	Wisconsin	251	251	0.54	0.31	153	0.87	0.50		174	20.21	8.83	93 3.69 2.63

Table 10: Detailed comparison results of ROBLIGHT, GNNEV, and SCIP-MPNN for weak and general robustness on the Cora, CiteSeer, Cornell, Texas, and Wisconsin datasets with various aggregation functions with global and local budgets $\Delta = 10$. Note that SCIP-MPNN only implements weak robustness for **sum** aggregation. t_a denotes the average runtime, and t_g denotes the shifted geometric mean of the runtime.

		ROBLIGHT				GNNEV				SCIP-MPNN			
		All instances		Robust instances		All instances		Robust instances		All instances		Robust instances	
		#Instances	#Solved	$t_a(s)$	$t_g(s)$	#Instances	#Solved	$t_a(s)$	$t_g(s)$	#Instances	#Solved	$t_a(s)$	$t_g(s)$
sum (Weak)	Cora	2708	2,680	1.93	0.62	2,119	2.22	0.74		1,679	19.21	8.85	1,214 16.28 6.46
	CiteSeer	3312	3,286	0.47	0.13	2,890	0.53	0.15		2,982	13.18	7.08	2,597 11.16 5.78
	Cornell	183	183	0.03	0.02	84	0.07	0.05		158	12.34	7.39	67 11.68 5.14
	Texas	183	181	3.44	0.76	141	3.16	0.48		142	11.19	4.80	112 7.03 2.77
	Wisconsin	251	235	0.22	0.16	186	0.27	0.19		180	15.20	7.53	135 10.10 4.63
sum	Cora	2708	2,698	1.18	0.33	1,448	1.71	0.50		2,000	21.72	10.27	964 12.22 4.27
	CiteSeer	3312	3,291	0.19	0.08	2,431	0.26	0.10		3,063	17.11	8.25	2,214 13.68 5.71
	Cornell	183	183	0.01	0.01	72	0.01	0.01		171	11.29	7.74	61 8.94 4.50
	Texas	183	183	0.02	0.02	77	0.05	0.04		162	9.53	5.57	57 1.26 1.09
	Wisconsin	251	248	0.52	0.23	154	0.50	0.23		206	20.80	9.80	119 9.12 4.29
max	Cora	2708	2,631	3.61	1.05	1,464	5.56	1.65		1,706	85.07	26.61	876 10.77 4.49
	CiteSeer	3312	3,278	0.73	0.22	2,474	0.87	0.26		2,652	64.49	17.35	1,958 20.98 8.76
	Cornell	183	182	0.38	0.14	91	0.75	0.28		140	39.90	18.13	59 18.39 7.15
	Texas	183	176	0.15	0.08	135	0.19	0.10		127	24.87	8.18	99 5.70 2.66
	Wisconsin	251	237	4.48	0.95	166	6.13	1.27		142	58.16	13.21	105 11.76 5.31
mean	Cora	2708	2,706	0.63	0.15	1,422	0.93	0.23		1,848	22.83	11.48	837 7.41 3.14
	CiteSeer	3312	3,296	0.27	0.10	2,463	0.31	0.12		2,880	13.14	7.40	2,082 9.40 4.89
	Cornell	183	183	0.14	0.10	99	0.21	0.14		146	12.78	7.48	67 6.29 3.69
	Texas	183	181	0.52	0.13	101	0.94	0.24		152	12.19	6.03	73 6.33 2.26
	Wisconsin	251	246	1.31	0.44	143	2.21	0.73		178	14.92	8.20	93 3.63 2.59

Table 11: Detailed comparison results of ROBLIGHT and SCIP-MPNN for weak and general robustness on the MUTAG and ENZYMES datasets with various aggregation functions with global budget $\Delta = 1$ and local budgets $\delta = 1$. Note that SCIP-MPNN only implements weak robustness for **sum** aggregation. t_a denotes the average runtime, and t_g denotes the shifted geometric mean of the runtime.

		ROBLIGHT				SCIP-MPNN					
		All instances		Robust instances		All instances		Robust instances			
		#Instances	#Solved	$t_a(s)$	$t_g(s)$	#Solved	$t_a(s)$	$t_g(s)$	#Solved	$t_a(s)$	$t_g(s)$
sum (Weak)	MUTAG	188	188	0.01	0.01	53	0.03	0.03	104	285.14	236.39
	ENZYMES	600	600	0.14	0.13	354	0.21	0.21	121	233.41	159.82
sum	MUTAG	188	188	0.01	0.01	53	0.03	0.03			
	ENZYMES	600	600	0.08	0.07	109	0.29	0.28			
max	MUTAG	188	188	0.01	0.01	3	0.01	0.01			
	ENZYMES	600	600	0.01	0.01	49	0.03	0.03			
mean	MUTAG	188	188	0.03	0.03	111	0.05	0.05			
	ENZYMES	600	600	0.27	0.23	183	0.70	0.61			

Table 12: Detailed comparison results of ROBLIGHT and SCIP-MPNN for weak and general robustness on the MUTAG and ENZYMES datasets with various aggregation functions with global budget $\Delta = 2$ and local budgets $\delta = 1$. Note that SCIP-MPNN only implements weak robustness for **sum** aggregation. t_a denotes the average runtime, and t_g denotes the shifted geometric mean of the runtime.

		ROBLIGHT				SCIP-MPNN					
		All instances		Robust instances		All instances		Robust instances			
		#Instances	#Solved	$t_a(s)$	$t_g(s)$	#Solved	$t_a(s)$	$t_g(s)$	#Solved	$t_a(s)$	$t_g(s)$
sum (Weak)	MUTAG	188	188	0.03	0.02	2	1.87	1.73	61	210.07	123.20
	ENZYMES	600	591	9.35	3.76	114	38.56	21.41	52	120.58	60.49
sum	MUTAG	188	188	0.03	0.02	2	1.85	1.71			
	ENZYMES	600	598	2.15	0.84	24	21.11	11.84			
max	MUTAG	188	188	0.01	0.01	0	N/A	N/A			
	ENZYMES	600	600	0.61	0.14	17	15.91	2.77			
mean	MUTAG	188	188	1.32	1.14	71	3.29	3.07			
	ENZYMES	600	584	6.20	2.15	43	27.91	12.02			

Table 13: Detailed comparison results of ROBLIGHT and SCIP-MPNN for weak and general robustness on the MUTAG and ENZYMES datasets with various aggregation functions with global budget $\Delta = 2$ and local budgets $\delta = 2$. Note that SCIP-MPNN only implements weak robustness for **sum** aggregation. t_a denotes the average runtime, and t_g denotes the shifted geometric mean of the runtime.

		ROBLIGHT				SCIP-MPNN					
		All instances		Robust instances		All instances		Robust instances			
		#Instances	#Solved	$t_a(s)$	$t_g(s)$	#Solved	$t_a(s)$	$t_g(s)$	#Solved	$t_a(s)$	$t_g(s)$
sum (Weak)	MUTAG	188	188	0.03	0.03	2	2.40	2.18	76	39.47	11.67
	ENZYMES	600	591	9.81	3.77	90	48.21	26.81	55	84.76	32.26
sum	MUTAG	188	188	0.04	0.03	2	2.47	2.24			
	ENZYMES	600	598	2.18	0.83	23	20.01	10.60			
max	MUTAG	188	188	0.01	0.01	0	N/A	N/A			
	ENZYMES	600	600	0.63	0.15	17	16.59	2.88			
mean	MUTAG	188	188	1.51	1.24	42	6.20	5.98			
	ENZYMES	600	584	6.58	2.12	33	27.61	12.94			

Table 14: Detailed comparison results of ROBLIGHT and SCIP-MPNN for weak and general robustness on the MUTAG and ENZYMES datasets with various aggregation functions with global budget $\Delta = 5$ and local budgets $\delta = 1$. Note that SCIP-MPNN only implements weak robustness for **sum** aggregation. t_a denotes the average runtime, and t_g denotes the shifted geometric mean of the runtime.

		ROBLIGHT						SCIP-MPNN						
		All instances			Robust instances			All instances			Robust instances			
		#Instances	#Solved	$t_a(s)$	$t_g(s)$	#Solved	$t_a(s)$	$t_g(s)$	#Solved	$t_a(s)$	$t_g(s)$	#Solved	$t_a(s)$	$t_g(s)$
sum	MUTAG	188	188	0.10	0.07	1	8.96	8.96	63	139.06	78.47	0	N/A	N/A
	ENZYMES	600	542	6.55	2.15	6	0.64	0.56	108	89.03	52.18	3	46.86	29.38
sum	MUTAG	188	188	0.10	0.07	1	8.96	8.96						
	ENZYMES	600	590	1.86	0.53	3	1.11	1.01						
max	MUTAG	188	188	0.01	0.01	0	N/A	N/A						
	ENZYMES	600	590	0.32	0.13	7	10.83	3.81						
mean	MUTAG	188	155	5.88	1.76	0	N/A	N/A						
	ENZYMES	600	561	6.45	1.99	7	50.71	12.48						

Table 15: Detailed comparison results of ROBLIGHT and SCIP-MPNN for weak and general robustness on the MUTAG and ENZYMES datasets with various aggregation functions with global budget $\Delta = 5$ and local budgets $\delta = 2$. Note that SCIP-MPNN only implements weak robustness for **sum** aggregation. t_a denotes the average runtime, and t_g denotes the shifted geometric mean of the runtime.

		ROBLIGHT						SCIP-MPNN						
		All instances			Robust instances			All instances			Robust instances			
		#Instances	#Solved	$t_a(s)$	$t_g(s)$	#Solved	$t_a(s)$	$t_g(s)$	#Solved	$t_a(s)$	$t_g(s)$	#Solved	$t_a(s)$	$t_g(s)$
sum	MUTAG	188	188	0.22	0.20	0	N/A	N/A	65	22.90	8.22	0	N/A	N/A
	ENZYMES	600	537	7.01	2.18	4	0.01	0.01	133	31.23	15.76	2	40.27	20.17
sum	MUTAG	188	188	0.22	0.20	0	N/A	N/A						
	ENZYMES	600	589	1.22	0.44	2	0.01	0.01						
max	MUTAG	188	188	0.01	0.01	0	N/A	N/A						
	ENZYMES	600	589	0.37	0.11	6	9.24	3.82						
mean	MUTAG	188	186	11.18	4.36	0	N/A	N/A						
	ENZYMES	600	568	6.01	2.03	3	15.12	7.69						

Table 16: Detailed comparison results of ROBLIGHT and SCIP-MPNN for weak and general robustness on the MUTAG and ENZYMES datasets with various aggregation functions with global budget $\Delta = 5$ and local budgets $\delta = 5$. Note that SCIP-MPNN only implements weak robustness for **sum** aggregation. t_a denotes the average runtime, and t_g denotes the shifted geometric mean of the runtime.

		ROBLIGHT						SCIP-MPNN						
		All instances			Robust instances			All instances			Robust instances			
		#Instances	#Solved	$t_a(s)$	$t_g(s)$	#Solved	$t_a(s)$	$t_g(s)$	#Solved	$t_a(s)$	$t_g(s)$	#Solved	$t_a(s)$	$t_g(s)$
sum	MUTAG	188	188	0.29	0.25	0	N/A	N/A	109	53.29	21.68	0	N/A	N/A
	ENZYMES	600	535	8.30	2.64	5	0.01	0.01	203	116.51	50.24	2	47.47	22.48
sum	MUTAG	188	188	0.29	0.26	0	N/A	N/A						
	ENZYMES	600	587	1.58	0.68	5	0.01	0.01						
max	MUTAG	188	188	0.01	0.01	0	N/A	N/A						
	ENZYMES	600	591	0.31	0.12	5	20.46	6.82						
mean	MUTAG	188	188	16.68	4.78	0	N/A	N/A						
	ENZYMES	600	575	5.06	1.76	3	40.37	13.59						